AD NUMBER: AD0456328

LIMITATION CHANGES

TO:

Approved for public release; distribution is unlimited.

FROM:

Distribution authorized to US Government Agencies only; Administrative/Operational Use; 1 Dec 1964. Other requests shall be referred to Chief, Bureau of Ships, Washington, DC, 20350.

AUTHORITY

BUSHIPS ltr dtd 17 May 1965

Technical Report

Low-Cycle Fatigue of Experimental HY-130/150 and HY-180/210 Steels and Weldments

Applied Research Laboratory
United States Steel
Monroeville, Pennsylvania

December 1, 1964 Project No. 40.018-001(37)

NObs-88540 SR007-01-01 Task 853 S-13307-1
S-13308
S-23308-1

LOW-CYCLE FATIGUE OF EXPERIMENTAL HY-130/150 AND HY-180/210 STEELS AND WELDMENTS

(40.018-001)(37)(a-ORD-NP-3)(S-13307-1, S-13308, and S-23308-1)

By S. T. Rolfe, R. P. Haak, and E. J. Imhof, Jr.

Approved by J. H. Gross, Division Chief

Abstract

Because submarine hulls are cyclically loaded at high stresses, the fatigue behavior of experimental submarine-hull steels is important in evaluating their structural suitability. Therefore, the Applied Research Laboratory determined the low-cycle high-strain fatigue properties of the 5Ni-Cr-Mo-V experimental HY-130/150 steel, the 12Ni-5Cr-3Mo experimental HY-180/210 steel, and HY-80 steel, the current submarine-hull steel. In addition, the fatigue behavior of weldments of the 5Ni-Cr-Mo-V and HY-80 steels was determined, and the fatigue data for the unwelded specimens were analyzed in terms of recent theories proposed by Langer, Manson, and Morrow for predicting low-cycle fatigue behavior.

The results showed that in the cycle-life range of primary interest (10^4 to 10^5 cycles), the fatigue strength (strain range to cause failure) of the 5Ni-Cr-Mo-V and 12Ni-5Cr-3Mo steels was significantly higher than that of HY-80 steel. However, to insure a corresponding resistance to failure by fatigue, the fatigue strength of submarine-hull materials should be proportional to the yield strength of the material. On this basis, the fatigue strength of the 5Ni-Cr-Mo-V steel is slightly lower than that of HY-80 steel at a life of 10,000 cycles and essentially the same at 100,000 cycles, whereas the fatigue strength of the 12Ni-5Cr-3Mo steel is lower than that of HY-80 steel at all cycle lives. On the same yield-strength basis, the 5Ni-Cr-Mo-V steel covered-electrode weldments had a fatigue strength at 10,000 cycles slightly lower and a fatigue strength at 100,000 cycles slightly higher than that of the HY-80 steel covered-electrode weldments. The fatigue strength of the 5Ni-Cr-Mo-V steel MIG weldments was superior to that of the HY-80 steel covered-electrode weldments at 10,000 and 100,000 cycles.

The fatigue analysis proposed by Morrow agrees better with the experimental values than the analysis proposed by Langer or Manson because Morrow's predictory equations are based on experimental fatigue data, whereas Langer and Manson predict fatigue performance from tensile properties.

The results indicate that in the cycle range of primary interest, the fatigue properties of the 5Ni-Cr-Mo-V steel and weldments are surprisingly good and should permit design on the same yield-strength basis as that currently employed for HY-80 steel and weldments.

Introduction

Because submarine hulls are cyclically loaded at high stresses, the fatigue behavior of experimental submarine-hull steels is important in evaluating their structural suitability. Therefore, the Applied Research Laboratory determined the low-cycle high-strain fatigue properties of the 5Ni-Cr-Mo-V experimental HY-130/150 steel, the 12Ni-5Cr-3Mo experimental HY-180/210 steel, and HY-80 steel, the current submarine-hull steel.

The present report describes the results of the study, including the development of a new welded fatigue specimen, and analzes the results in terms of recent theories for predicting low-cycle fatigue behavior.

Materials and Experimental Work

The materials used in the present study were 1-inch-thick plates of HY-80, 5Ni-Cr-Mo-V, and 12Ni-5Cr-3Mo steels that were produced on commercial facilities. The check chemical analysis of the plates is given in Table I, and the mechanical properties are summarized in Tables II and III.

The unwelded fatigue specimens were cantilever-beam specimens of the type developed at Lehigh University[1)]* and used by the Marine Engineering Laboratory[2)] and the Naval Research Laboratory.[3)] Figure 1 shows the dimensions of the specimen.

Eleven HY-80 steel, thirteen 5Ni-Cr-Mo-V steel, and twelve 12Ni-5Cr-3Mo steel unwelded specimens were machined and tested as subsequently

---

*See References.

described. In addition twelve unwelded specimens were machined from a 12Ni-5Cr-3Mo steel plate that had been aged to produce 13 percent reverted austenite.

So that the fatigue behavior of weldments could be evaluated, a welded fatigue specimen incorporating a full weld joint was developed for testing on the low-cycle fatigue machines. The essential features of the specimen, shown in Figure 2, are as follows:

1. The specimen is nominally the same width as the unwelded specimen and thus provides the transverse restraint required to initiate cracks at the midwidth of the specimen.

2. The test section of the specimen is tapered so that the strain field is uniform over a 3-inch length (except as noted below). Thus, a transverse weld can be located in the center of a uniform strain field so that the strain imposed on the base metal, weld metal, and heat-affected zone is uniform.

3. A large (6 inch) radius (0.10 inch deep per side) is cut across the width of the specimen to localize the failure in the vicinity of the weld. Strain-gage measurements along the length of the specimen vary only 5 percent in strain over the center 1-1/2 inches of the specimen.

Fatigue tests of standard unwelded plate specimens and tapered unwelded plate specimens resulted in essentially identical lives. Thus, fatigue tests of weldments made with the specimen illustrated in Figure 2

can be compared directly with fatigue tests of standard unwelded plate specimens, Figure 1.

Nine welded HY-80 steel specimens from a covered-electrode weldment, ten welded 5Ni-Cr-Mo-V steel specimens from a covered-electrode weldment, and six welded 5Ni-Cr-Mo-V steel specimens from an inert-gas-shielded metal-arc weldment were machined and tested as subsequently described. The fabrication of the weldments is described in Table IV.

The fatigue machines, shown in Figure 3, are similar to those used at the Marine Engineering Laboratory.[4] The machines are hydraulically operated, and the fatigue tests were conducted at 10 to 20 cycles per minute in air. Strain gages were mounted on the reduced section of the specimens and the output fed into an X-Y recorder. The output from strain gages on weigh bars, which measured the load applied to the test specimen, was also fed into the X-Y recorder to obtain a complete applied moment - strain curve, as shown on the recorder in Figure 3. The total strain range was measured during the first 100 cycles, and the strain range at 10 cycles was used as the total strain range for any particular test. (The change of less than five percent observed in the total strain range with number of cycles of loading greater than 10 was not considered to be significant, although this change is being studied.) After the strain range had been established, the strain gage was removed and a fine insulated copper wire was cemented to the surface to act as a crack detector. Failure was defined as a 3/16-inch-long

surface crack. Procedures for the calculation of the elastic and plastic components of the total strain range are described in Appendix A.

Results and Discussion

Unwelded-Plate Fatigue Results

Detailed results of the cantilever-beam fatigue tests of the unwelded plate specimens of the three steels are presented in Appendix Tables A, B, and C, and the total strain range to failure of the three steels is compared in Figure 4 with a regression-analysis curve reported[2] by M. R. Gross (Marine Engineering Laboratory) that describes the performance of HY-80 steel.

The results show that, compared with HY-80 steel, the 5Ni-Cr-Mo-V and 12Ni-5Cr-3Mo steels both exhibit similar total strain ranges to failure below 10^3 cycles and higher strain ranges at lives between 10^3 and 10^5 cycles. For lives greater than 10^3 cycles, the total strain range is related to strength level in that the 12Ni-5Cr-3Mo steel (yield strength = 195 ksi) and the 5Ni-Cr-Mo-V steel (yield strength = 141 ksi) exhibited a greater strain range to failure than HY-80 steel (yield strength = 90.6 ksi).

Because ductility has been observed to be the controlling factor at low cycles[4,5,6,7], the strain range to failure for the higher strength steels was expected to be somewhat lower than that for HY-80 steel below 10^3 cycles. These expectations were not confirmed, as shown in Figure 4, and the excellent fatigue performance was attributed to the excellent cleanliness and ductility of these steels, particularly the 5Ni-Cr-Mo-V steel.

To study the effect of reverted austenite on the low-cycle fatigue behavior of a 12Ni-5Cr-3Mo steel, plates were heat treated to obtain about 13 percent reverted austenite. The results, Figure 5 and Table V, show no effect of reverted austenite on the low-cycle fatigue behavior of the 12Ni-5Cr-3Mo steel.

Weldment Fatigue Results

Results of tests conducted with HY-80 and 5Ni-Cr-Mo-V steel tapered welded fatigue specimens are listed in Table VI and compared with the regression-analysis curve for HY-80 steel in Figure 6. As illustrated in Figure 6 and summarized in Table VI, failure occurred in the weld metal except for three failures in the heat-affected zone. The results indicate that the values of strain range to failure for the HY-80 and 5Ni-Cr-Mo-V weldments lie in a band parallel to the band including the strain-range values for the corresponding unwelded plates but displaced downward. Thus the fatigue strength of both HY-80 and the 5Ni-Cr-Mo-V steel weldments is a little lower than the corresponding values for unwelded specimens.

Comparative Fatigue Performance

An estimate of the relative fatigue strength of the steels investigated can be obtained by comparing their strain range to failure at appropriate cycle lives. From Figure 4 and Figure 6, the strain-range values at 10,000 and 100,000 cycles (the cycle range of primary interest) were selected and the values for the various unwelded and welded materials are listed in Table VII.

At 10,000 cycles the strain range to failure for the 5Ni-Cr-Mo-V steel was about 1.29 times that of HY-80 steel. This is significantly lower than the ratio of the yield strength of the 5Ni-Cr-Mo-V steel to that of the HY-80 steel (1.56). Thus at 10,000 cycles, the ratio of the fatigue strength of the 5Ni-Cr-Mo-V steel to that of HY-80 steel was somewhat lower than the ratio of their yield strengths. At 100,000 cycles the strain range to failure for the 5Ni-Cr-Mo-V steel was about 1.56 times that of the HY-80 steel. This value is identical with the yield-strength ratio and indicates that the fatigue strength of the 5Ni-Cr-Mo-V steel at 100,000 cycles scales up in proportion to its yield strength. This is surprisingly good fatigue performance inasmuch as an increase in yield strength is not usually accompanied by a corresponding increase in fatigue strength. The fatigue strength of the 12Ni-5Cr-3Mo steel compared with that of HY-80 steel did not scale up in the same ratio as did the yield strength at 10,000 cycles (1.51 versus 2.15) or at 100,000 cycles (1.79 versus 2.15). However, this deficiency may be minimized as additional experience is gained in the production of the 12Ni-5Cr-3Mo steel.

The fatigue strength of the welded 5Ni-Cr-Mo-V steel also appeared quite good compared with that of HY-80 steel. Because failure of the welded samples occurred primarily in the weld metal for the welded HY-80 and the 5Ni-Cr-Mo-V steel specimens, the fatigue strength should be compared with the yield strength of their respective weld metals. The fatigue strength of

the 5Ni-Cr-Mo-V steel weldment was somewhat poorer at 10,000 cycles (1.09 versus 1.29) and somewhat better at 100,000 cycles (1.50 versus 1.29) on a yield-strength basis than that of the HY-80 steel weldment. For the 5Ni-Cr-Mo-V steel MIG weldment, the fatigue strength was slightly better at 10,000 cycles (1.29 versus 1.23) and markedly better at 100,000 cycles (1.77 versus 1.23) on a yield-strength basis than that of the HY-80 steel weldment.

The results generally indicate that the fatigue design stress based on fatigue strength proportional to the yield strength might be slightly lower for the 5Ni-Cr-Mo-V steel at a fatigue life of 10,000 cycles and about the same at 100,000 cycles compared with that for HY-80 steel. For weldments, the corresponding fatigue design stress of a 5Ni-Cr-Mo-V weldment would be about the same at 10,000 cycles and significantly higher at 100,000 cycles than that of an HY-80 steel weldment.

Analytical Results

Several methods based on the elastic and plastic components of the total strain range have been developed for analyzing fatigue data.[4,5,6,7] Most of these methods are based on results of axial fatigue tests in which the elastic and plastic components can be easily determined. However, for cantilever-beam specimens strained by bending, such as those used in the present investigation, the determination of the elastic and plastic components of strain must include an analysis of the residual stress induced by plastic straining.

As part of this investigation, a procedure was developed that takes account of the residual stresses produced in cantilever-beam fatigue specimens loaded into the plastic strain range. Briefly (the complete procedure is described in the Appendix), the apparent plastic strain obtained from the hysteresis loop (Appendix Figure A) is corrected for the residual stress resulting from non-uniform yielding of a rectangular bar. Assuming elastic unloading, the procedure described in the Appendix correctly includes any inelastic strain resulting from the Bauschinger effect as plastic strain.

Calculations of the elastic and plastic components of the total strain range are presented in Appendix tables D, E, and F and are summarized in Table IV for HY-80 steel, 5Ni-Cr-Mo-V steel, and 12Ni-5Cr-3Mo steel. These data were analyzed by using expressions developed by Langer[4], Manson[5], and Morrow[6] to predict the low-cycle fatigue behavior of materials. A brief description of each of these procedures using the data summarized in Table IV is presented in the following sections.

Langer's Fatique Analysis

Using Coffin's[7] basic equation, $N^{\frac{1}{2}} \epsilon_p = \frac{\epsilon_f}{2}$ (where N is the number of cycles, ϵ_p is the plastic fatigue strain, and ϵ_p is the true fracture strain measured in a tension test), Langer[4] noted that since the total strain component is comprised of the elastic and plastic components of total strain, the stress amplitude, S, could be written in terms of the elastic

stress component and plastic stress component (a fictitious value that assumes elastic behavior over the total strain range).

$$S = E\left(\frac{\epsilon_T}{2}\right) = E\ \frac{\epsilon_p}{2} + E\ \frac{\epsilon_e}{2} \qquad (1)$$

$$S = \frac{E}{4\sqrt{N}}\ \ln\left[\frac{100}{100-RA}\right] + \Delta S \qquad (2)$$

where S = total stress amplitude

E = modulus of elasticity

ϵ_T = total strain range

N = cycles to failure

$\ln\left[\frac{100}{100-RA}\right] = \epsilon_f$ = fracture ductility in tension test (true strain at fracture)

RA = percent reduction of area in tensile test

ΔS = elastic stress amplitude

Since ΔS is a function of N, Langer proposed that a more realistic model would result if ΔS were replaced by the fatigue limit, S_e. Thus as $N \rightarrow \infty$, $S \longrightarrow S_e$.

Since Langer assumed $S = \frac{E\epsilon_T}{2}$, Equation 2 can be rewritten in terms of the total strain as follows:

$$\epsilon_T = \frac{1}{2\sqrt{N}}\ \ln\left[\frac{100}{100-RA}\right] + \frac{2\ S_e}{E} \qquad (3)$$

By using modulus of elasticity (E) values of 30, 29, and 28 x 10^6 psi; fatigue limits (S_e stress amplitude in reversal) of 65, 100, and 110 ksi; and reduction of area values of 75.9, 71.0, and 61.8 percent for HY-80, 5Ni-Cr-Mo-V, and 12Ni-5Cr-3Mo steels, respectively, to predict ϵ_T in accordance with Equation 3, the actual results (Table IV) and predicted results (Equation 3) are compared in Figure 8.

The predictive curves calculated from Langer's equation cross between 10^3 and 10^4 cycles for the three steels; that is, the lowest strength, most ductile steel (HY-80) has a greater total strain range at low cycles (less than 10^3) than the stronger, less ductile steels, whereas the stronger steels (5Ni-Cr-Mo-V and 12Ni-5Cr-3Mo) have a greater strain range at high cycles (more than 10^4) than the weaker, more ductile HY-80 steel. The experimental values fall below the predictive curves because the criterion for failure in the predictive equation is complete separation, whereas the criterion for failure in bending tests was a 3/16-inch-long surface crack. Thus Langer's predictions include the crack propagation lives whereas the actual fatigue lives are only for crack initiation.

Manson's Fatique Analysis

Manson[5] has developed linear log-log relationships between the elastic strain range or the plastic strain range and the number of cycles to failure. These empirical relations are based on data obtained from conventional tension tests and correlated with axial fatigue tests for

various materials including steels, aluminum, and titanium. His empirical relations are as follows:

$$\epsilon_T = \epsilon_e + \epsilon_p$$

$$(\epsilon_e)_{N=1/4} = 2.5 \frac{\sigma_f}{E}$$

$$(\epsilon_e)_{N=10^5} = 0.90 \frac{\sigma_{ult}}{E}$$

$$(\epsilon_e)_{N=10} = 1/4(\epsilon_f)^{3/4}$$

$$(\epsilon_p)_{N=10^4} = 0.01 - (\epsilon_e)_{N=10^4}$$

(determine $(\epsilon_e)_{N=10^4}$ from ϵ_e - N curve)

where ϵ_T = total strain range

ϵ_e = elastic strain range

ϵ_p = plastic strain range

N = number of cycles to failure

σ_f = true fracture stress (no Bridgeman correction)

E = modulus of elasticity

σ_{ult} = ultimate tensile strength

ϵ_f = true fracture strain $(\ln \frac{A_o}{A})$

By using the above relations and data from Tables II and III, ϵ_e at N = 1/4 and at N = 10^5 was calculated and the ϵ_e curves were plotted, Figure 9. Similarly, the ϵ_p curves were plotted from calculated values of

ϵ_p at N = 10 and at N = 10^4. The respective ϵ_e and ϵ_p curves were algebraically summed to obtain the ϵ_T curves for HY-80, 5Ni-Cr-Mo-V, and 12Ni-5Cr-3Mo steel. Experimental data from Table IV are also plotted. Although the data (Table IV) fit Manson's predictions (Figure 9) better than Langer's predictions (Figure 8) at long lives, the experimental values again fall below the theoretical curves for lives between 10^2 and 10^4 and for the same reason mentioned in the section on Langer's analysis.

Morrow's Fatigue Analysis

Morrow[6] has shown that cyclic hardening or softening of a material can occur during fatigue testing and that cyclic stress-strain properties should therefore be used to predict fatigue results rather than monotonic stress-strain results. (An example of the difference in stress (moment)-strain curves for 1 and 10 cycles for HY-80, 5Ni-Cr-Mo-V, and 12Ni-5Cr-3Mo steels is presented in Appendix Figure E). Thus, on the basis of cyclic stress-strain properties, Morrow developed linear log-log relations between elastic or plastic strain and number of reversals of loading. (Manson's relationships were similar but based on monotonic stress-strain curves).

Morrow's general expression is:

$$\Delta\epsilon_T = \Delta\epsilon_p + \Delta\epsilon_e$$

$$\Delta\epsilon_T = 2\epsilon_{f1}\,(2N_f)^c + \frac{2\sigma_{f1}}{E}\,(2N_f)^h \qquad (4)$$

where: $\Delta\epsilon_T$ = total strain range

$\Delta\epsilon_p$ = plastic strain range

$\Delta\epsilon_e$ = elastic strain range

$2\epsilon_f^1$ = intercept of the log $\Delta\epsilon_p$ versus log $2N_f$ curve at $2N_f = 1$.

ϵ_f^1 is the fatigue-ductility coefficient

$2N_f$ = number of reversals or half cycles to failure

c = fatigue ductility exponent; slope of the $\log\Delta\epsilon_p$ versus log $2N_f$ curve

σ_f^1 = fatigue-strength coefficient; intercent of the $\log\sigma a$ versus log $2N_f$ curve at $2N_f = 1$

E = modulus of elasticity

$\underline{2\sigma_f^1}$ = intercept of the $\log\Delta\epsilon_e$ versus log $2N_f$ curve at $2N_f = 1$

b = fatigue strength exponent; Basquins exponent; the slope of the $\log\sigma a$ versus log $2N_f$ plot or the $\log\Delta\epsilon_e$ versus log $2N_f$ curve

The corresponding elastic strains ($\Delta\epsilon_e$) and cycle lives (N) from Table IV were plotted in Figure 10, 11, and 12 to establish the $\Delta\epsilon_e$ curves for the three steels. From the curves, the intercept value, $\frac{2\sigma_f^1}{E}$, and the slope of the curve, b, were determined for each steel. By using these

values, the generalized $\Delta\epsilon_e$ equation for each steel was established as shown in Figures 10, 11, and 12.

By the same procedure, except that $\Delta\epsilon_p$ values rather than $\Delta\epsilon_e$ values were plotted, the intercept value, $2\Delta\epsilon_f$[1], and the slope of the curve, c, were determined for each steel and the generalized $\Delta\epsilon_p$ equation for each steel was established as shown in Figures 10, 11, and 12. Finally, the generalized $\Delta\epsilon_T$ equation for each steel was established by substituting various reversal values into Equation 4. Alternately the $\Delta\epsilon_T$ curve can be drawn by adding the $\Delta\epsilon_e$ and $\Delta\epsilon_p$ curves in Figures 10, 11, and 12.

As shown in Figures 10, 11, and 12, the experimental $\Delta\epsilon_T$ values agree very well with the $\Delta\epsilon_T$ curve, as indeed they must, inasmuch as the $\Delta\epsilon_T$ curve is a summation of the $\Delta\epsilon_e$ and $\Delta\epsilon_p$ curves, which in turn are established from the experimental $\Delta\epsilon_e$ and $\Delta\epsilon_p$ values. In essence, Morrow's equations show (as did Manson's equations) that the relation between the total strain range, $\Delta\epsilon_T$, and the cycles to failure is not a linear log-log relation, whereas $\Delta\epsilon_e$ versus N and $\Delta\epsilon_p$ versus N are linear log-log relations. By determining the elastic and plastic components of the total strain and drawing the respective $\Delta\epsilon_e$ and $\Delta\epsilon_p$ curves, a more precise extrapolation of the $\Delta\epsilon_T$ curve can be obtained than would be obtained if a straight line were to be drawn through several $\Delta\epsilon_{T-N}$ values on a log-log plot. The procedure devised by Morrow would be more precise than that of Langer or Manson for establishing the $\Delta\epsilon_T$ curve when only a small number of $\Delta\epsilon_{T-N}$ values are

available and when the curve is to be extrapolated beyond the range for which the values have been determined.

Of the three methods employed for analyzing the experimentally obtained fatigue data, Morrow's procedure best agreed with the experimental determinations because it was based on the experimental fatigue data themselves and did not attempt to predict fatigue behavior from tension-test results. On the other hand, Manson's analysis is extremely useful because the fatigue performance is predicted from tensile properties, and Langer's analysis of fatigue performance requires knowledge only of the fatigue limit and the reduction of area of the steel.

Summary

The results of an investigation to determine the low-cycle fatigue behavior of experimental HY-130/150 and HY-180/210 steels and weldments may be summarized as follows:

1. When the fatigue strength of HY-80, 5Ni-Cr-Mo-V, and 12Ni-5Cr-3Mo steels are compared on a yield-strength basis, the fatigue strength of the 5Ni-Cr-Mo-V steel is slightly lower than that of HY-80 steel at a life of 10,000 cycles and essentially the same as that of HY-80 steel at 100,000 cycles, whereas the fatigue strength of the 12Ni-5Cr-3Mo steel is lower than that of HY-80 steel at all cycle lives.

2. On the same yield-strength basis, the 5Ni-Cr-Mo-V steel covered-electrode weldments had a fatigue strength at 10,000 cycles slightly

lower and a fatigue strength at 100,000 cycles slightly higher than that of the HY-80 steel covered-electrode weldments. The fatigue strength of the 5Ni-Cr-Mo-V steel MIG weldments was superior to that of the HY-80 steel covered-electrode weldments at 10,000 and at 100,000 cycles.

3. The fatigue analysis proposed by Morrow agrees better with the experimental values than the analysis proposed by Langer or Manson because Morrow's analysis is based on empirically derived equations whereas Langer and Manson predict fatigue performance from tensile properties.

The results indicate that in the cycle range of primary interest, the fatigue properties of the 5Ni-Cr-Mo-V steel and weldments are surprisingly good and should permit design on the same yield-strength basis as that currently employed for HY-80 steel and weldments.

Recommendations and Future Work

Corrosion fatigue and notched fatigue tests of unwelded plates and weldments are currently in progress.

References

1. J. H. Gross, S. Tsang, and R. D. Stout, "Factors Affecting Resistance of Pressure-Vessel Steels to Repeated Overloading," Welding Journal, Vol. 32, No. 1 (January 1953), 23-s to 30-s.

2. M. R. Gross, "Low Cycle Fatigue of Materials for Submarine Construction," Naval Engineers Journal, 1963, p. 783.

3. P. P. Puzak, et al., "Metallurgical Characteristics of High Strength Structural Materials," (Third Quarterly Report), U. S. Naval Research Laboratory Report No. 6086, January 1964.

4. B. F. Langer, "Design of Pressure Vessels for Low-Cycle Fatigue," Trans. ASME, Vol. 84, 1962, p. 389.

5. S. S. Manson and M. H. Hirschberg, "Fatigue Behavior in Strain Cycling in the Low- and Intermediate-Cycle Range," Fatigue—An Interdisciplinary Approach, Proceedings of the Tenth Sagamore Army Materials Research Conference, edited by J. J. Burke, N. L. Reed, and V. Weiss, Syracuse University Press, 1964.

6. J. Morrow and F. R. Tuler, "Low Cycle Fatigue Evaluation of Inconel 713C and Waspaloy, ASME Preprint No. 64-MET-15, 1964.

7. L. F. Coffin, Jr. "A Study of the Effects of Cyclic Thermal Stresses on a Ductile Metal," Trans. ASME, Vol. 76, 1954, p. 931.

APPENDIX

APPENDIX

Calculation of Elastic and Plastic Strain Ranges

General

Several parameters can be determined directly from the load-strain curves obtained for each specimen. These include:

ϵ_T = total strain range

M_{TA} = actual total moment range - 10 P_t
where P_t = total load range

$\epsilon_{P'}$ = plastic strain based on offset of stress-strain curve

These parameters are shown in Figure A, which is a typical load-strain curve for cantilever beam fatigue specimens tested in bending.

Theoretical Total Moment, M_{TT}

For a rectangular section loaded in bending beyond the yield point, the theoretical total moment is:

$$M_{TT} = 2\left[2\int_0^c (\sigma\ w\ dy)\ y\right] \qquad (1)$$

where $c = \frac{\text{specimen depth}}{2} = 0.25$ inches

σ = stress at any section

w = specimen width = 2.5 inches

y = moment arm about neutral axis

Tensile stress-strain curves for HY-80, 5Ni-Cr-Mo-V, and 12Ni-5Cr-3Mo steels are shown in Figure B. Compressive stress-strain curves have

similar shapes, although the yield strengths are slightly higher as shown below:

Steel	Tensile Yield	Compressive Yield	Average
HY-80	90.6	94.0	92
5Ni-Cr-Mo-V	141.4	150.0	146
12Ni-5Cr-3Mo	195.0	216.8	206

As shown in Figure B, assuming a flat-top, stress-strain curve introduces only a small error at yield-point strains, which is essentially compensated for at larger strain values by neglecting strain hardening. Thus to determine the theoretical moment in the elastic-plastic region, a flat-top stress-strain curve with yield strength equal to the average of the tensile and compressive yield was chosen.

Strain-gage measurements show that the fatigue specimens are subjected to a biaxial stress system of 2:1 ($\sigma_1 = 2\sigma_2$). Since yield strength for $\frac{\sigma_2}{\sigma_1} = 1/2$ is about 15 percent greater than the uniaxial yield strength from tension tests (octahedral shear stress or energy of distortion theories of failure), a somewhat higher yield strength than the uniaxial tensile yield stress should be used. Only half the theoretical increase (15%) over the uniaxial yield stress was used since the restraint necessary to give 2:1 biaxial loading does not exist over the entire width of the specimen. Thus, the yield strength of the fatigue specimens was assumed to be 1.07 times the

uniaxial yield strength (average of tensile and compressive yield strength). Thus Equation 1 can be written as:

$$M_{TT} = 4\,w\left[\int_{o}^{a} \sigma\, y\, dy + \int_{a}^{c} \sigma\, y\, dy\right] \qquad (2)$$

where a = distance from neutral axis to start of plastic region (obtained graphically by assuming linear strain distribution)

$$\sigma = 1.07\sigma_{ys}\left(\frac{y}{a}\right) \quad \text{for } 0 \leq y \leq a$$

$$\sigma = 1.07\sigma_{ys} \quad \text{for } a \leq y \leq c$$

σ_{ys} = average of uniaxial tension and compression yield strengths

Therefore:

$$M_{TT} = 4\,w\left[\frac{1.07\sigma_{ys}}{a}\int_{o}^{a} y^2\, dy + 1.07\sigma_{ys}\int_{a}^{c} y\, dy\right]$$

$$M_{TT} = 2\,\frac{w(1.07\sigma_{ys})}{3}\left[3c^2 - a^2\right]$$

For strain ranges less than yield strain, the actual stress was calculated and substituted into Equation 3 for $1.07\sigma_{ys}$.

Values of the actual total moment (M_{TA}) and the theoretical total moment (M_{TT}) are tabulated in Appendix Tables A, B, and C for the steels investigated. As shown in these tables and in Figure C, excellent agreement was obtained between the actual and theoretical total moment. Thus, the shape of the assumed stress block for each specimen is apparently correct and can be used to determine the actual plastic strain range.

Because of the excellent agreement between the actual and theoretical total moments, the size of the elastic core (2a) must likewise be correct. By using this value of a, and the fact that a residual stress exists at zero bending moment on unloading of a beam that has yielded, a correction* is applied to the measured plastic strain range (ϵ_p') to obtain the true plastic strain range. This correction assumes that unloading is elastic; and therefore inelastic strain resulting from the Bauschinger effect is correctly classified as plastic strain.

On unloading to zero moment from the total theoretical moment, a stress equal to $\frac{MC}{I}$ must be subtracted from the yield stress ($1.07\sigma_{ys}$) to obtain the residual stress. Thus,

$$\sigma_r = 1.07\sigma_{ys} - \frac{MC}{I}$$

$$\sigma_r = 1.07\sigma_{ys} - \frac{3}{2wc^2}$$

$$\text{where } M = w\,\frac{(1.07\sigma_{ys})}{3}\left[3c^2 - a^2\right]$$

$$\text{or } \sigma_r = \frac{1.07\sigma_{ys}}{2}\left[\left(\frac{a}{c}\right)^2 - 1\right] \qquad (4)$$

Converting stresses to strains and since:

$$\epsilon_p' = \epsilon_p + 2\epsilon_r$$

Then ϵ_p = actual plastic strain = $\epsilon_p' - 2\epsilon_r$

$$\epsilon_p = \epsilon_p' - 1.07\epsilon_y\left[\left(\frac{a}{c}\right)^2 - 1\right] \qquad (5)$$

*G. R. Halford, Private Communication

Values of the corrected plastic and elastic strain ranges are presented in Tables D, E, and F. The results are summarized in Figure D where the total elastic strain range is plotted versus the actual total moment. As expected, the elastic strain range is proportional to the moment up to the yield moment. Beyond the yield moment, the elastic strain range should remain constant if there were no change in the moment-strain relationships as a result of cyclic loading. As shown in Figure D, changes apparently do occur for the larger values of total moment since the strains corresponding to these values of moment are higher than the yield strain.

Moment-versus-strain curves for the first cycle of loading and the tenth cycle of loading are shown in Figure E. The curves for the first cycle of loading were from a single specimen loaded well into the plastic range. The curves for the tenth cycle are composites of the end points of moment-strain curves $(\frac{M_{TA}}{2})$ versus $\frac{\epsilon_T}{2}$ for several specimens.

A single specimen was cycled ten times and then loaded well into the plastic region in an attempt to define the moment-strain curve after 10 cycles. However, because of residual stresses and the Bauschinger effect, the curve was much lower than the hysterisis loop until the end points were reached; also the zero point on the curve was difficult to establish. Work is continuing on this problem.

From these curves, Figure E, it can be seen that at the higher moment ranges, the strain range at 10 cycles is greater than the strain range

at 1 cycle. This would be expected since for constant deflection tests, the strain range is known to increase with increasing numbers of cycles of loading. However, the hysterisis loop generally stabilizes after about 10 cycles of loading.

Figure E shows that the elastic strain range increases at higher values of applied moment and thus the total elastic strain values shown in Figure D should be above the initial yield strain for higher values of applied moment. Expressions that take account of the actual stress-strain curve of the material are being investigated.

Table A

Actual and Theoretical Data for HY-80 Steel

Specimen Number	ϵ_t, inches/inch x 10^6	N Cycles	ϵ_p' From Stress-Strain Curve, inches/inch x 10^6	M_{TA}, inch-pounds	$\epsilon_{T/2}$, inches/inch x 10^6	σ, psi	a, inches	M_{TT}, inch-pounds
8-9	5000	37,519	0	16,100	2500	75,000	0.25	15,600
8-6	5800	39,088	100	16,700	2900	87,000	0.25	18,100
8-7	6500	13,294	300	19,300	3250	97,500	0.25	20,300
8-13	8080	7206	1000	20,400	4040	98,500	0.203	24,000
8-8	10,450	2516	2400	25,400	5225	98,500	0.158	26,600
8-3	13,100	1553	3900	26,200	6550	98,500	0.125	28,000
8-4	15,840	712	6100	27,300	7920	98,500	0.103	28,800
8-5	20,000	379	9400	28,200	10,000	98,500	0.082	29,500
8-14	22,320	280	11,200	29,000	11,160	98,500	0.073	29,800
8-12	24,120	320	12,700	30,100	12,060	98,500	0.067	30,000
8-2	25,000	291	13,800	30,900	12,500	98,500	0.065	30,000

Table B

Actual and Theoretical Data for 5Ni-Cr-Mo-V Steel

Specimen Number	ϵ_t, inches/inch x 10^6	N Cycles	ϵ_p, From Stress-Strain Curve, inches/inch x 10^6	M_{TA}, inch-pounds	$\epsilon_{T/2}$, inches/inch x 10^6	σ_f', psi	a, inches	M_{TT}, inch-pounds
5N-45	6500	80,880	0	19,300	3250	94,300	0.25	19,600
5N-47	7000	42,500	0	21,100	3500	101,000	0.25	21,000
5N-34	8140	17,510	0	24,900	4070	118,000	0.25	24,600
5N-25	10,000	11,800	200	30,300	5000	145,000	0.25	30,200
5N-35	10,080	6458	200	30,100	5040	146,000	0.25	30,400
5N-31	11,770	2870	300	34,100	5880	156,000	0.231	34,800
5N-36	12,210	2150	600	35,000	6100	156,000	0.222	35,800
5N-26	13,900	1860	1200	37,200	6950	156,000	0.195	38,700
5N-28	15,350	1770	2600	37,400	7670	156,000	0.176	40,500
5N-29	16,000	1195	2600	38,700	8000	156,000	0.169	41,300
5N-30	18,460	740	3200	41,400	9230	156,000	0.146	43,200
5N-27	21,500	450	6000	44,100	10,750	156,000	0.125	44,400
5N-38	25,000	281	7900	45,300	12,500	156,000	0.108	45,500

Table C

Actual and Theoretical Data for 12Ni-5Cr-3Mo Steel

Specimen Number	ϵ_t, inches/inch x 10^6	N Cycles	$\epsilon_{p'}$ From Stress-Strain Curve, inches/inch x 10^6	M_{TA}, inch-pounds	$\epsilon_{T/2}$, inches/inch x 10^6	σ, psi	a, inches	M_{TT}, inch-pounds
12N-12	7520	69,200	0		3760	105,000	0.25	21,900
12N-21	7900	48,667	0	23,500	3950	110,500	0.25	23,000
12N-2	9000	23,074	0	26,700	4500	126,000	0.25	26,200
12N-17	9500	18,661	0	27,200	4750	133,000	0.25	27,900
12N-24	9970	9400	0	28,700	4980	139,000	0.25	28,800
12N-20	11,000	6930	0	32,000	5500	154,000	0.25	32,100
12N-19	12,040	4210	0	36,500	6020	168,500	0.25	35,100
12N-16	13,020	2470	0	38,100	6510	182,000	0.25	37,900
12N-14	13,800	2275	0	38,600	6900	193,000	0.25	40,200
12N-1	15,680	1056	0	43,000	7840	219,000	0.25	45,600
12N-22	21,000	315	2400	52,700	10,500	220,000	0.188	55,600
12N-23	28,000	120	6700	60,500	14,000	220,000	0.140	61,200

Table D

Determination of Elastic Strain Range for HY-80 Steel

Specimen Number	a, inches	$\left[\left(\frac{a}{c}\right)^2 - 1\right]$	1.07 ϵ_y, inches/inch x 10^6	$_2\epsilon_r$, inches/inch x 10^6	ϵ_p', inches/inch x 10^6	ϵ_p, inches/inch x 10^6	ϵ_T, inches/inch x 10^6	$\epsilon_T - \epsilon_p = \epsilon_e$, inches/inch x 10^6
8-9	0.25	0	3280	0	0	0	5000	5000
8-6	0.25	0	3280	0	100	100	5800	5700
8-7	0.25	0	3280	0	300	300	6500	6200
8-13	0.203	-0.34	3280	-1120	1000	2120	8080	5960
8-8	0.158	-0.60	3280	-1970	2400	4370	10,450	6080
8-3	0.125	-0.75	3280	-2460	3900	6360	13,100	6740
8-4	0.103	-0.83	3280	-2720	6100	8820	15,840	7020
8-5	0.082	-0.89	3280	-2920	9400	12,320	20,000	7680
8-14	0.073	-0.91	3280	-2980	11,200	14,180	22,320	8140
8-12	0.067	-0.93	3280	-3050	12,700	15,750	24,120	8370
8-2	0.065	-0.93	3280	-3050	13,800	16,850	25,000	8150

Table E

Determination of Elastic Strain Range for 5Ni-Cr-Mo-V Steel

Specimen Number	a, inches	$\left[\left(\frac{a}{c}\right)^2 - 1\right]$	$1.07\,\epsilon_y$, inches/inch x 10^6	$2\epsilon_r$, inches/inch x 10^6	ϵ_p', inches/inch x 10^6	ϵ_p, inches/inch x 10^6	ϵ_T, inches/inch x 10^6	$\epsilon_T - \epsilon_p = \epsilon_e$ inches/inch x 10^6
5N-45	0.25	0	5400	0	0	0	6500	6500
5N-47	0.25	0	5400	0	0	0	7000	7000
5N-34	0.25	0	5400	0	0	0	8140	8140
5N-25	0.25	0	5400	0	200	200	10,000	9800
5N-35	0.25	0	5400	0	200	200	10,080	9880
5N-31	0.231	-0.15	5400	-810	300	1110	11,770	10,660
5N-36	0.222	-0.21	5400	-1130	600	1730	12,210	10,480
5N-26	0.195	-0.39	5400	-2100	1200	3300	13,900	10,600
5N-28	0.176	-0.50	5400	-2700	2600	5300	15,350	10,050
5N-29	0.169	-0.54	5400	-2920	2600	5520	16,000	10,480
5N-30	0.146	-0.66	5400	-3560	3200	6760	18,460	11,700
5N-27	0.125	-0.75	5400	-4050	6000	10,050	21,500	11,450
5N-38	0.108	-0.81	5400	-4370	7900	12,270	25,000	12,730

Table F

Determination of Elastic Strain Range for 12Ni-5Cr-3Mo Steel

Specimen Number	a, inches	$\left[\left(\frac{a}{c}\right)^2 - 1\right]$	$1.07\epsilon_y$, inches/inch x 10^6	$2\epsilon_r$, inches/inch x 10^6	ϵ_p', inches/inch x 10^6	ϵ_p, inches/inch x 10^6	ϵ_T, inches/inch x 10^6	$\epsilon_T - \epsilon_p = \epsilon_e$, inches/inch x 10^6
12N-12	0.25	0	7880	0	0		7520	7520
12N-21	0.25	0	7880	0	0		7900	7900
12N-2	0.25	0	7880	0	0		9000	9000
12N-17	0.25	0	7880	0	0		9500	9500
12N-24	0.25	0	7880	0	0		9970	9970
12N-20	0.25	0	7880	0	0		11,000	11,000
12N-19	0.25	0	7880	0	0		12,040	12,040
12N-16	0.25	0	7880	0	0		13,020	13,020
12N-14	0.25	0	7880	0	0		13,800	13,800
12N-1	0.25	0	7880	0	0		15,680	15,680
12N-22	0.188	-0.44	7880	-3470	2400	5870	21,000	15,130
12N-23	0.140	-0.69	7880	-5440	6700	12,140	28,000	15,860

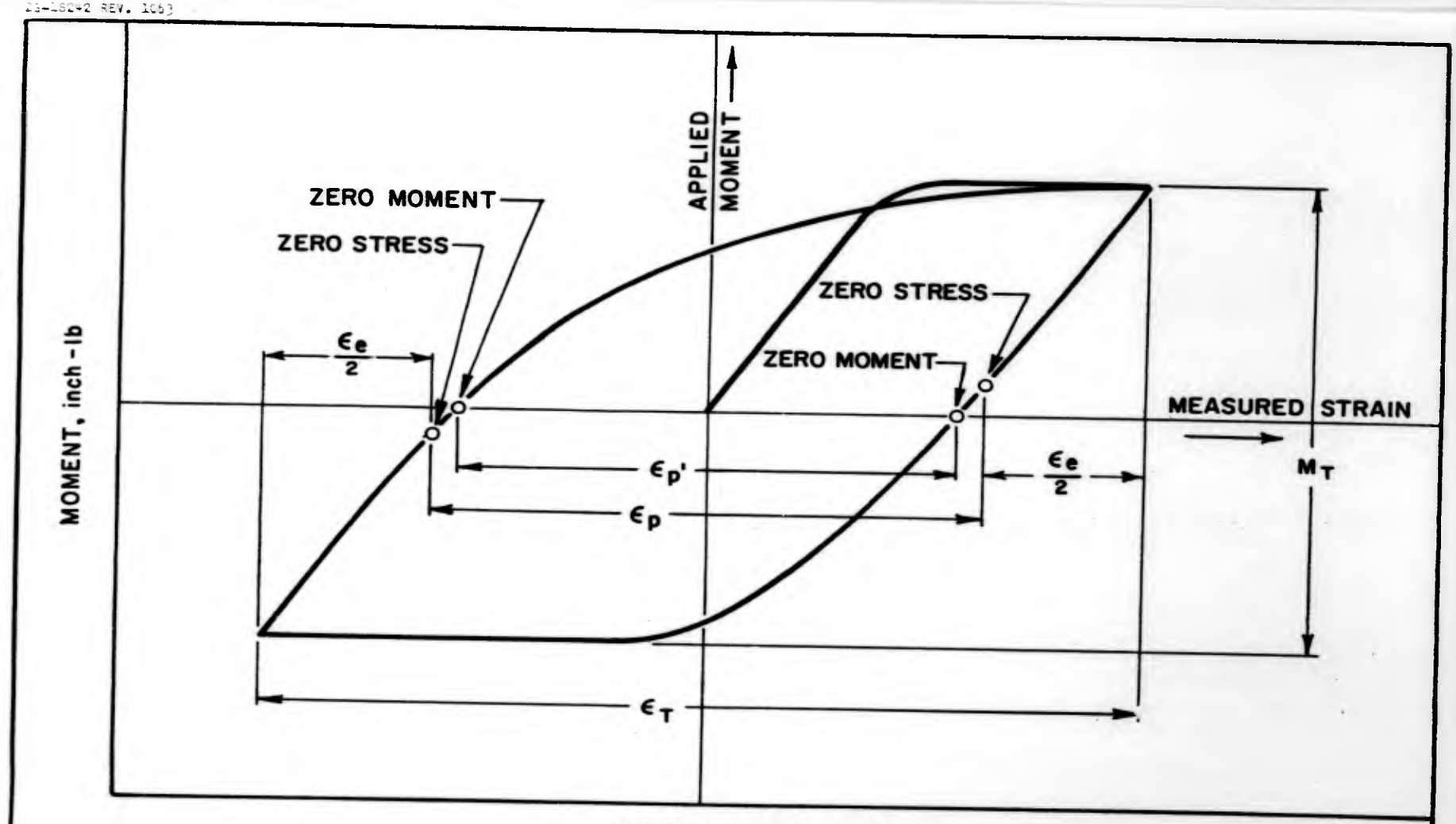

TYPICAL MOMENT–STRAIN CURVE

DRAWN BY	CHK'D BY	APPROVED BY	UNITED STATES STEEL CORPORATION	FIGURE NO.
G.A.Z.	S.T.R.	J.H.G.	APPLIED RESEARCH	A
DRAWING NO		PROJECT No	PITTSBURGH, PA.	
ARL 18-468		40 018-001 (37)		
		DATE 11-12-64		

G-18242 REV. 1063

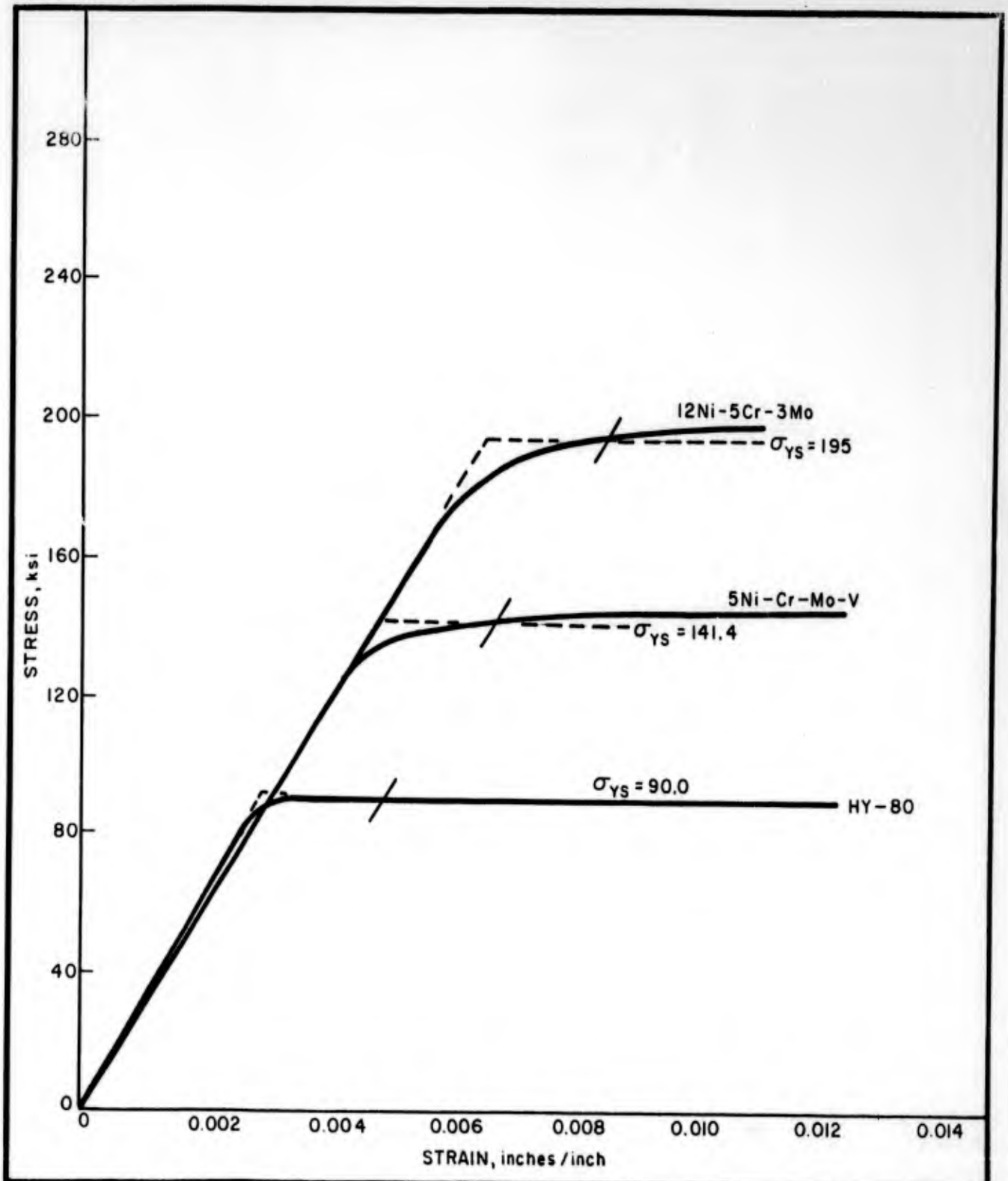

STRESS-STRAIN CURVES FOR HY-80, 5Ni-Cr-Mo-V, AND 12Ni-5Cr-3Mo STEELS

DRAWN BY	CHK'D BY	APPROVED BY	UNITED STATES STEEL CORPORATION	FIGURE NO.
G. A. Z.	S. T. R.	J. H. G.	APPLIED RESEARCH PITTSBURGH, PA.	B
DRAWING No.		PROJECT No.		
ARL 18-469		40.018-001 (37)		
		DATE		
		11-11-64		

ATLAS LITHO CO PGH PA 1028 CLEARPRINT

G-18242 REV. 1063

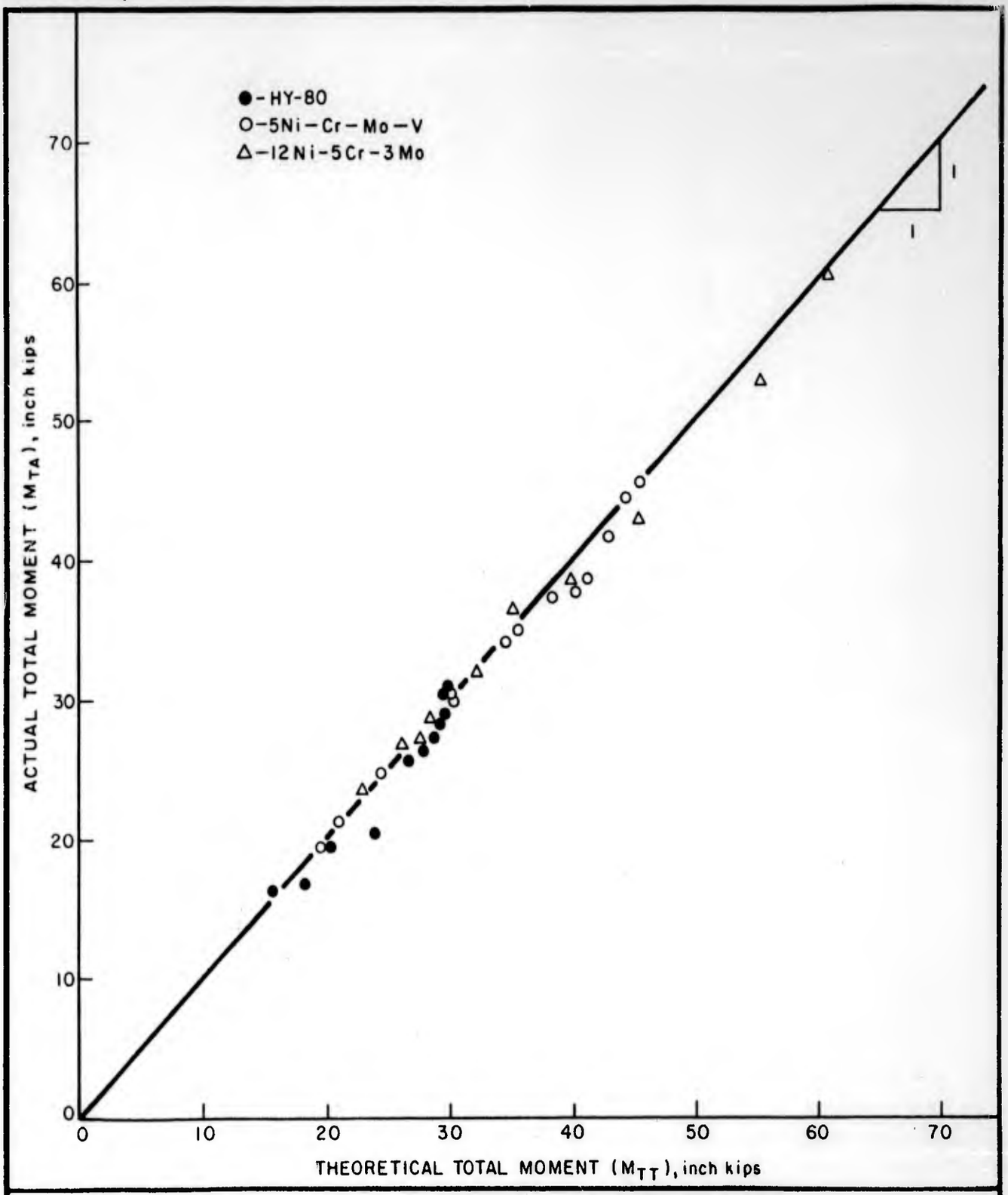

ACTUAL VERSUS THEORETICAL TOTAL MOMENT FOR
HY-80, 5Ni-Cr-Mo-V, AND 12Ni-5Cr-3Mo STEELS

DRAWN BY	CHK'D BY	APPROVED BY	UNITED STATES STEEL CORPORATION	FIGURE NO.
G.A.Z.	S.T.R.	J.H.G.	APPLIED RESEARCH PITTSBURGH, PA.	C
DRAWING No.		PROJECT No. 40.018-001 (37)		
ARL 18-470		DATE 11-10-64		

G-18242 REV. 1063

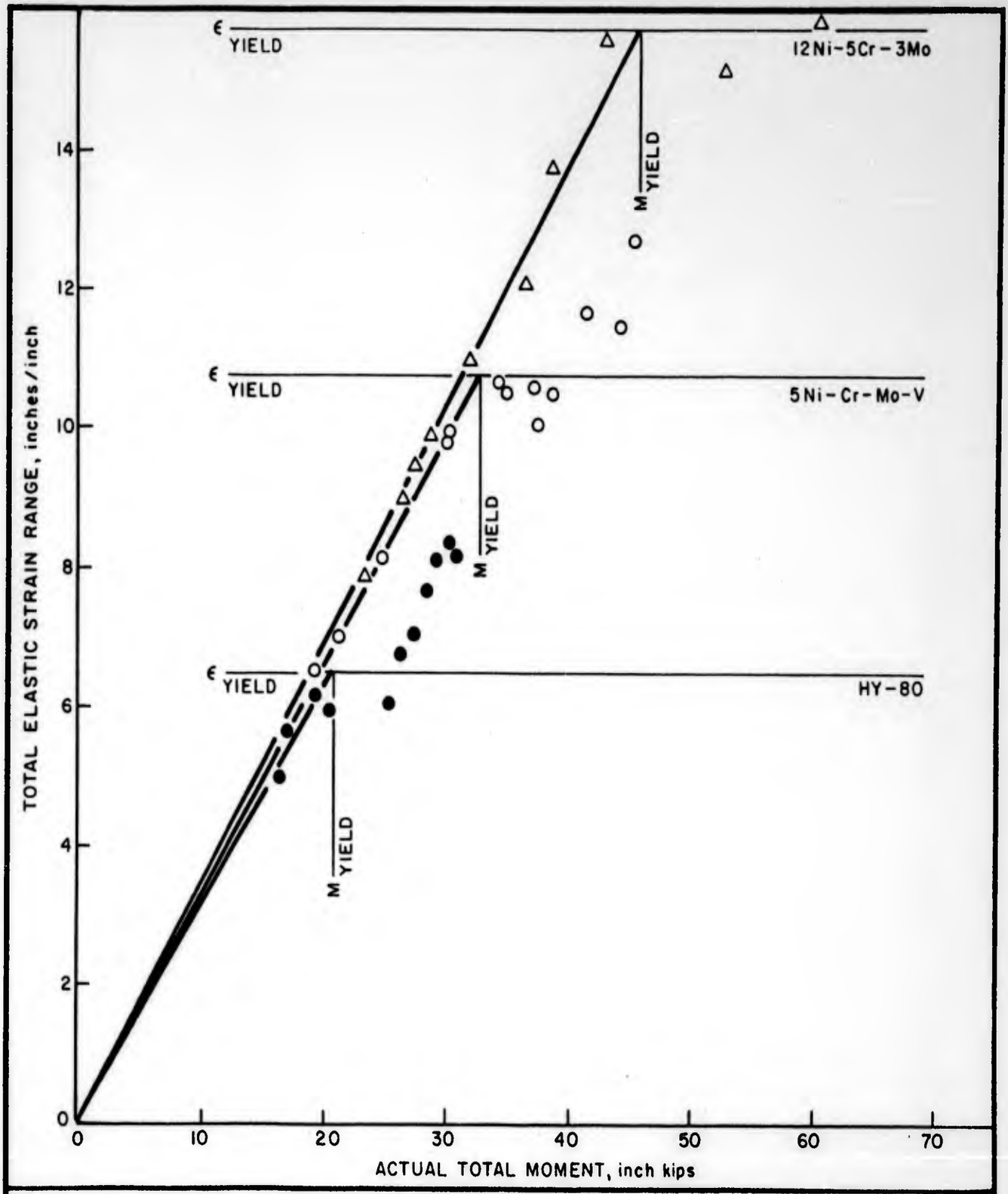

RELATION OF ELASTIC STRAIN TO MOMENT

DRAWN BY	CHK'D BY	APPROVED BY	UNITED STATES STEEL CORPORATION	FIGURE NO.
G.A.Z.	S.T.R.	J.H.G.	APPLIED RESEARCH	
DRAWING No		PROJECT No. 40.018-001 (37)	PITTSBURGH, PA.	D
ARL 18-471		DATE 11-10-64.		

ATLAS LITHO CO. PGH. PA. 1028 CLEARPRINT

G-18242 REV. 1063

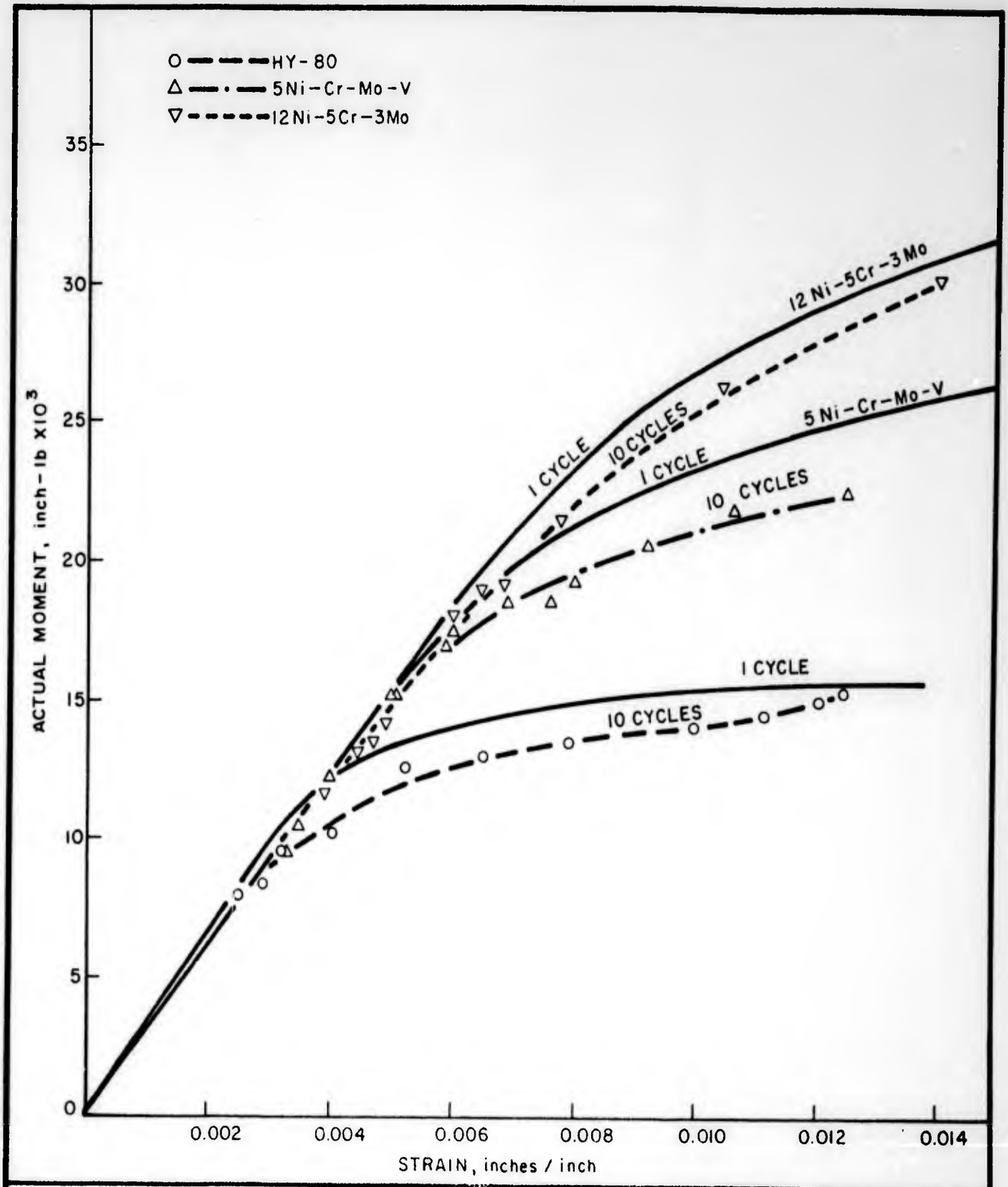

MOMENT-STRAIN CURVES AT 1 AND 10 CYCLES FOR HY-80, 5Ni-Cr-Mo-V, AND 12Ni-5Cr-3Mo STEELS

DRAWN BY	CHK'D BY	APPROVED BY	UNITED STATES STEEL CORPORATION	FIGURE NO.
G.A.Z.	S.T.R.	J.H.G.	APPLIED RESEARCH PITTSBURGH, PA.	E
DRAWING No		PROJECT No		
ARL 18-472		40 018-001 (37)		
		DATE		
		11-10-64		

610617

Table I

Chemical Composition of 1-Inch-Thick Plates of Steels Investigated—Percent
(Check Analyses)

Steel	Heat No.	C	Mn	P	S	Si	Ni	Cr	Mo	V	Al*	N**	Cu	Ti
HY-80[1]	66U471	0.17	0.26	0.012	0.018	0.24	2.33	1.16	0.25	<0.005	0.032	0.008	0.030	<0.005
5Ni-Cr-Mo-V[2]	X53185	0.10	0.72	0.007	0.005	0.28	5.03	0.60	0.54	0.07	0.017	0.01	—	—
12Ni-5Cr-3Mo[3]	X15339	0.024	0.044	0.007	0.013	0.042	11.74	5.38	3.18	—	0.47	0.008	—	0.30

*Acid soluble.
**Kjeldahl determination.

1) 300-ton open-hearth heat.
2) 80-ton electric-furnace heat.
3) 20-ton electric-furnace heat.

Table II

Mechanical Properties of Steels Investigated

Steel	Yield Strength (0.2% Offset), ksi	Tensile Strength, ksi	Reduction of Area, %		Elongation in 1 Inch, %	
			At Maximum Load	At Fracture	At Maximum Load	At Fracture
HY-80 Plain Plate	90.6	107	14.4	75.9	12.0	26.8
HY-80 Covered-Electrode Weld Metal	112.0	123	10.7	65.0	10.0	22.0
5Ni-Cr-Mo-V Plain Plate	141.0	147	10.7	71.0	8.5	20.8
5Ni-Cr-Mo-V MIG Weld Metal	138.0	149	10.0	67.7	7.5	20.0
5Ni-Cr-Mo-V Covered-Electrode Weld Metal	144.0	158	10.0	57.4	8.0	19.5
12Ni-5Cr-3Mo Plain Plate	195.0	199	2.8	61.8	2.5	15.0
12Ni-5Cr-3Mo Plain Plate With 13 Percent Reverted Austenite	171.0	179	7.8	62.3	6.2	16.8

Table III

True Stress-Strain Properties of Steels Investigated

Steel	True Stress, ksi		True Strain, ln $\frac{A_o}{A}$	
	At Maximum Load	At Fracture	At Maximum Load	At Fracture
HY-80 Plain Plate	123	245	0.14	1.43
HY-80 Covered-Electrode Weld Metal	139	234	0.113	1.03
5Ni-Cr-Mo-V Plain Plate	167	279	0.104	1.21
5Ni-Cr-Mo-V MIG Weld Metal	165	277	0.104	1.13
5Ni-Cr-Mo-V Covered-Electrode Weld Metal	175	259	0.088	0.855
12Ni-5Cr-3Mo Plain Plate	205	323	0.025	0.975
12Ni-5Cr-3Mo Plain Plate With 13 Percent Reverted Austenite	195	302	0.091	0.985

Table IV

Conditions Used to Fabricate 1-Inch-Thick Butt-Welded Fatique Specimens

Steel	Welding Process	Electrode	Electrode Diameter, inch	Current, amps	Voltage, volts	Arc Travel Speed, rpm	Preheat and Interpass Temperature, F	Total Number of Weld Reach
HY-80	Covered Electrode	AWS Class E11018-G	5/32 and 3/16	170 210	23 24	6 10	78	13
5Ni-Cr-Mo-V	Covered Electrode	Airco Experimental No. Z737*	5/32	175	23	6	200	15
5Ni-Cr-Mo-V	Automatic MIG**	Airco Experimental No. 9376*	1/16	320	29	14	200	16

*The nominal composition of the Airco experimental electrodes was 0.09C-2.0Mn-2.0Ni-0.8Cr-0.5Mo.

**The MIG shielding gas used was 50 cu ft per hour of argon plus 2% oxygen.

Table V

Summary of Fatigue Results for HY-80, 5Ni-Cr-Mo-V, and 12Ni-5Cr-3Mo Steels

Steel	Strain Ranges, inches/inch x 10^6 ϵ_e	ϵ_p	ϵ_T	Number of Cycles to Failure
HY-80	5000	0	5000	37,519
	5700	100	5800	39,088
	6200	300	6500	13,294
	5960	2120	8080	7206
	6080	4370	10,450	2516
	6740	6360	13,100	1553
	7020	8820	15,840	712
	7680	12,320	20,000	379
	8140	14,180	22,320	280
	8370	15,750	24,120	320
	8150	16,850	25,000	291
5Ni-Cr-Mo-V	6500	0	6500	80,880
	7000	0	7000	42,500
	8140	0	8140	17,510
	9800	200	10,000	11,800
	9880	200	10,080	6458
	10,660	1110	11,770	2870
	10,480	1730	12,210	2150
	10,600	3300	13,900	1860
	10,050	5300	15,350	1770
	10,480	5520	16,000	1195
	11,700	6760	18,460	740
	11,450	10,050	21,500	450
	12,730	12,270	25,000	281
12Ni-5Cr-3Mo	7520	0	7520	69,200
	7900	0	7900	48,667
	9000	0	9000	23,074
	9500	0	9500	18,661
	9970	0	9970	9400
	11,000	0	11,000	6930
	12,040	0	12,040	4210
	13,020	0	12,020	2470
	13,800	0	13,800	2275
	15,680	0	15,680	1056
	15,130	5870	21,000	315
	15,860	12,140	28,000	120

(40.018-001) (37)

Table VI

Fatigue Results for 12Ni-5Cr-3Mo
Steel with 13% Reverted Austenite

ϵ_T, inches/inch x 10^6	Number of Cycles to Failure
5,000	100,700 (No failure)
6,100	122,600 (No failure)
7,100	83,000
7,980	56,470
8,030	38,170
9,000	22,765
9,970	7,449
12,080	3,415
13,050	3,108
13,600	2,739
15,080	1,395
21,300	436

Table VII

Summary of Weldment Fatique Results

Weldment	ϵ_T inches/inch x 10^6	Number of Cycles to Failure	Location of failure
HY-80 Covered Electrode	4,000	23,272	Weld Metal
	6,040	5,345	Weld Metal
	6,060	1,520	Weld Metal
	8,040	1,400	Weld Metal
	8,090	4,432	HAZ
	10,120	1,521	Weld Metal
	13,000	200	Weld Metal
	16,100	390	HAZ
	19,200	120	Weld Metal
5Ni-Cr-Mo-V Covered Electrode	4,140	75,000	Weld Metal
	5,080	14,686	Weld Metal
	5,120	83,600	Weld Metal
	6,050	3,519	Weld Metal
	6,150	5,060	Weld Metal
	7,000	5,233	Weld Metal
	7,950	3,266	Weld Metal
	8,100	3,030	Weld Metal
	9,100	3,230	Weld Metal
	12,250	319	Weld Metal
5Ni-Cr-Mo-V MIG	5,130	63,200	Weld Metal
	6,500	11,730	Weld Metal
	7,460	10,132	Weld Metal
	8,080	9,600	Weld Metal
	10,300	765	Weld Metal
	11,900	1,211	HAZ

Table VIII

Comparative Fatique Performance for Steels Investiqated

Steel	Strain Range to Failure at Indicated Cycles, inches per inch		Ratio of Strain Range to Failure at Indicated Cycles to that for HY-80 Steel, inches per inch	
	10,000	100,000	10,000	100,000
Unwelded				
HY-80	0.0076	0.0039	—	—
5Ni-Cr-Mo-V	0.0098	0.0061	1.29	1.56
12Ni-5Cr-3Mo	0.0115	0.0070	1.51	1.79

Ratio of yield strength of 5Ni-Cr-Mo-V steel to that of HY-80 steel = 1.56

Ratio of yield strength of 12Ni-5Cr-3Mo steel to that of HY-80 steel = 2.15

Welded				
HY-80 (Covered Electrode)	0.0056	0.0026	—	—
5Ni-Cr-Mo-V (Covered Electrode)	0.0061	0.0039	1.09	1.50
5Ni-Cr-Mo-V (MIG)	0.0072	0.0046	1.29	1.77

Ratio of yield strength of 5Ni-Cr-Mo-V weld metal (covered electrode) to that of HY-80 weld metal (covered electrode) = 1.29

Ratio of yield strength of 5Ni-Cr-Mo-V weld metal (MIG) to that of HY-80 weld metal (covered electrode) = 1.23

2G-1824-2 REV. 2063

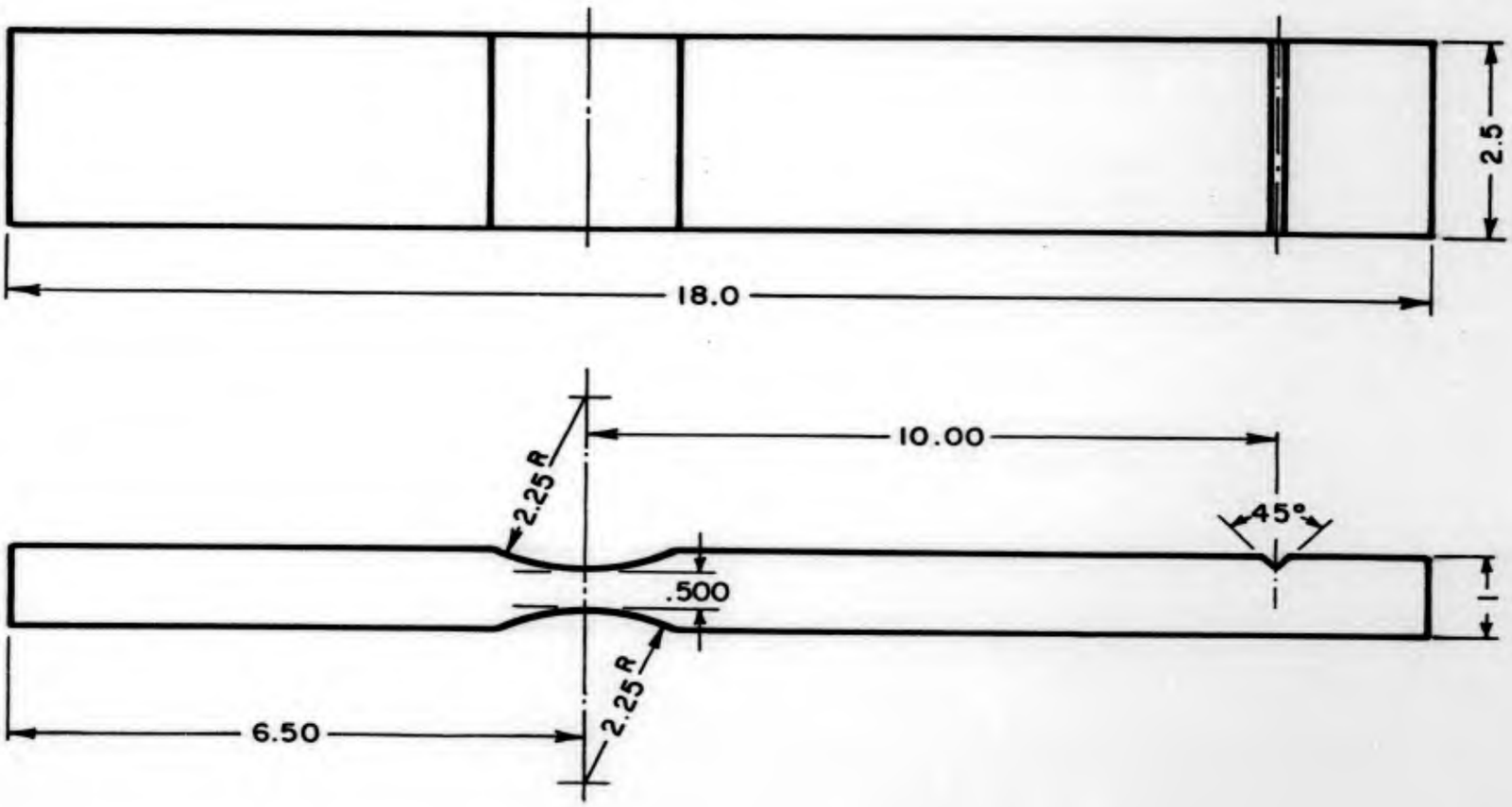

DETAILS OF UNWELDED LOW-CYCLE FATIGUE SPECIMEN

DRAWN BY	CHK'D BY	APPROVED BY	UNITED STATES STEEL CORPORATION	FIGURE NO.
G.A.Z.	S.T.R.	J.H.G.	APPLIED RESEARCH	
DRAWING NO		PROJECT NO	PITTSBURGH, PA.	
ARL 18-473		40.018-001 (37)		1
		DATE 11-11-64		

1025 Clearprint Pitt Photo Litho Co., Inc. Pgh., Pa.

2G-18242 REV. 1063

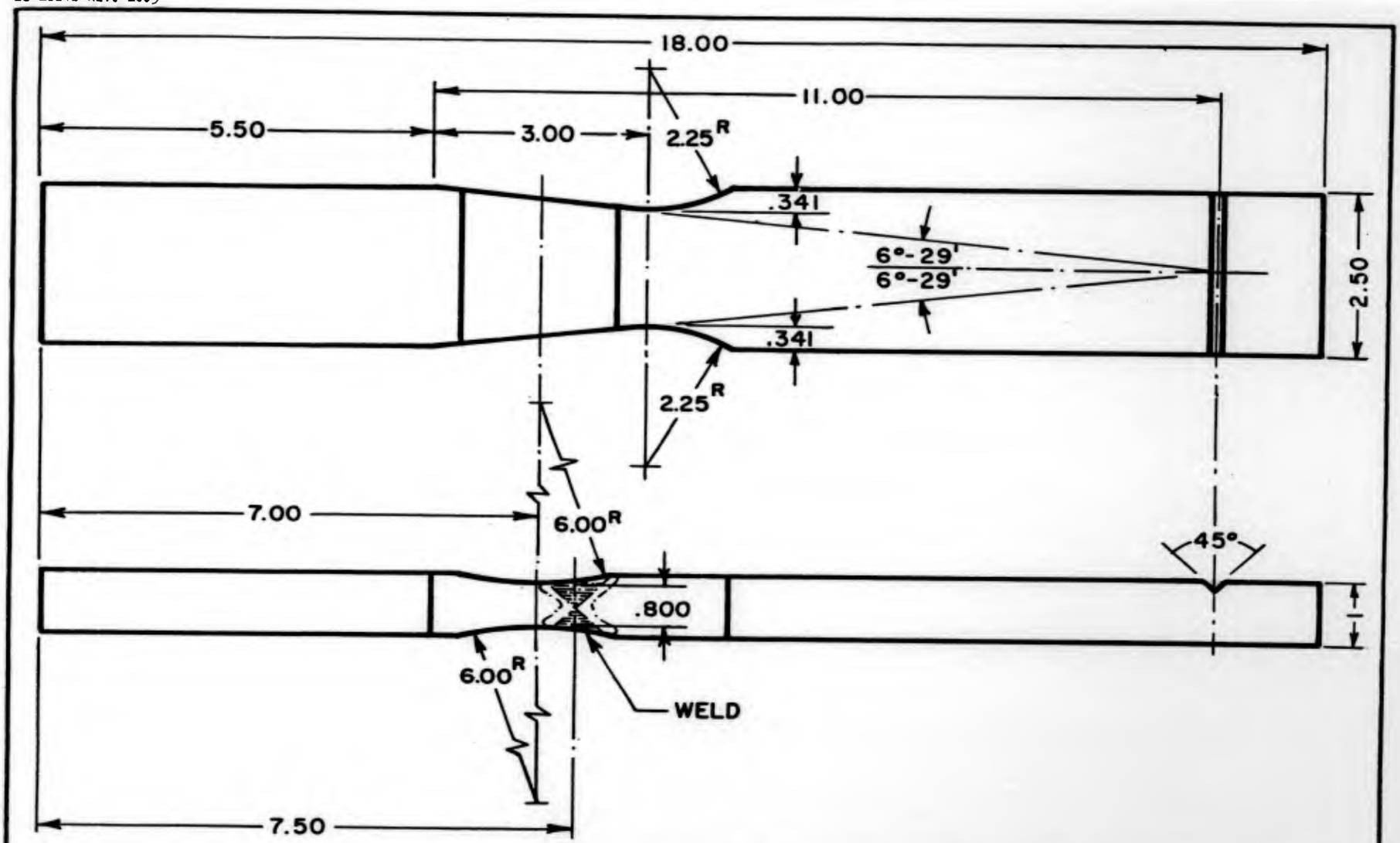

TAPERED WELDED LOW-CYCLE FATIGUE SPECIMEN

DRAWN BY	CHK'D BY	APPROVED BY	UNITED STATES STEEL CORPORATION APPLIED RESEARCH PITTSBURGH, PA.	FIGURE NO.
G.A.Z.	S.T.R.	J.H.G.		
DRAWING NO		PROJECT NO		
ARL 18-474		40.018-001(37)		2
		DATE		
		11-11-64		

1025 Clearprint Pitt Photo Litho Co., Inc. Pgh., Pa.

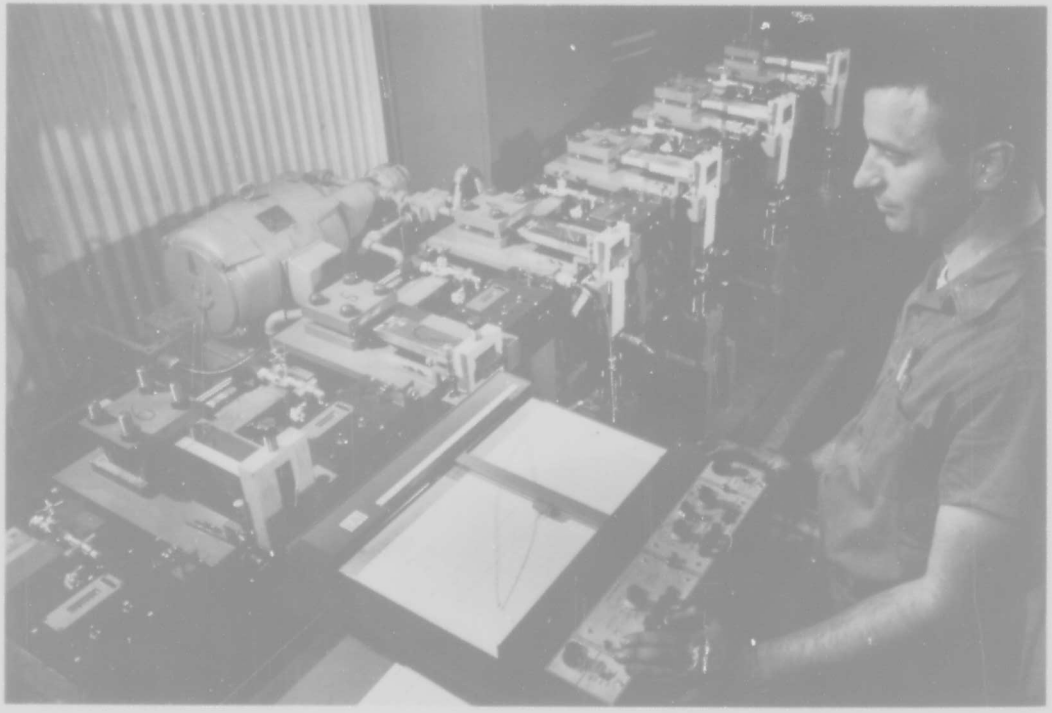

Figure 3. Low-cycle fatigue machines and X-Y recorder showing typical hysteresis loop.

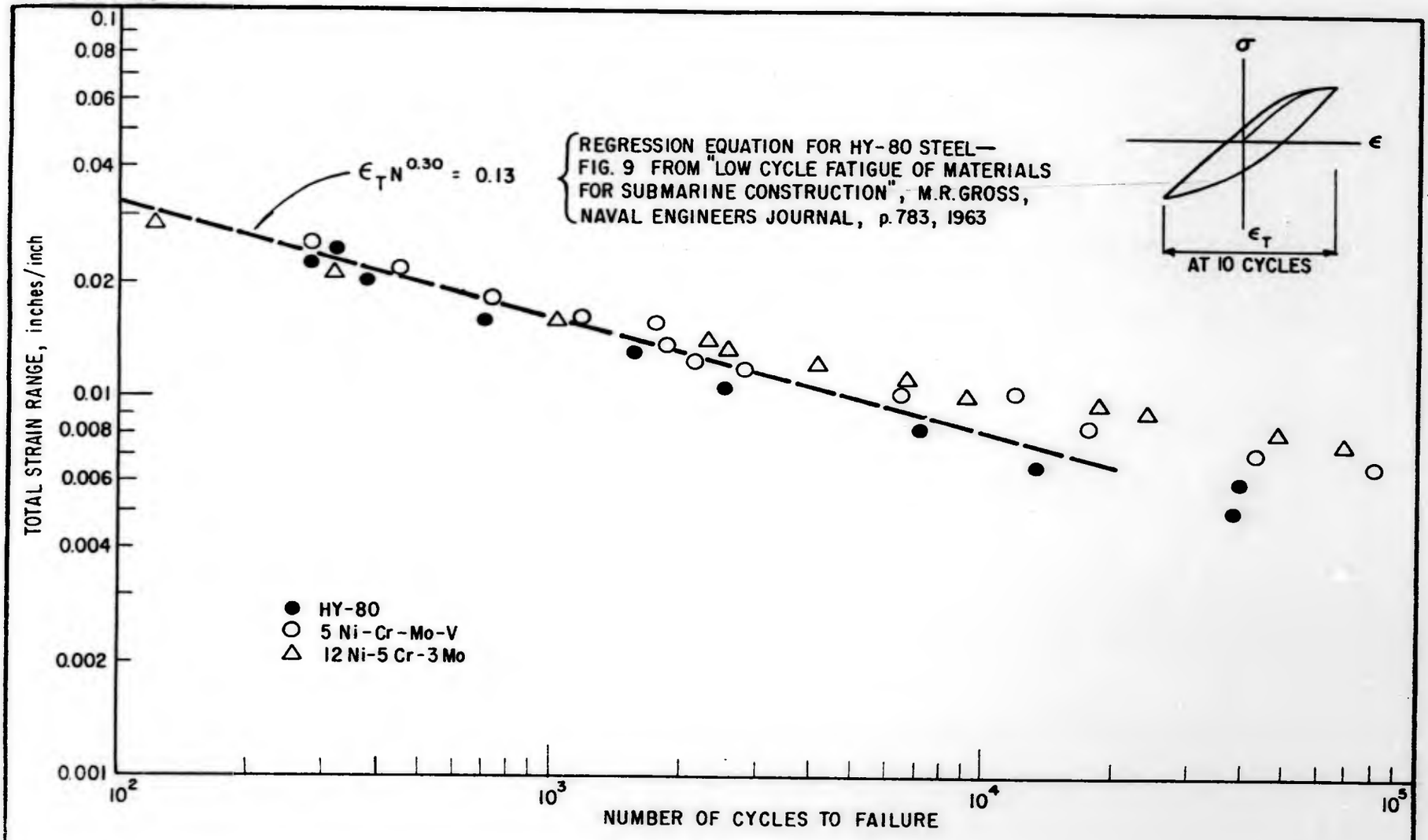

LOW-CYCLE FATIGUE RESULTS FOR 5 Ni-Cr-Mo-V, HY-80, AND 12 Ni-5 Cr-3 Mo STEELS

DRAWN BY	CHK'D BY	APPROVED BY
M.M.	S.T.R.	J. H. G.
DRAWING No	PROJECT No	
ARL 18-415	40.018-001 (37)	
	DATE 7/8/64	

UNITED STATES STEEL CORPORATION
APPLIED RESEARCH
PITTSBURGH, PA.

FIGURE NO. 4

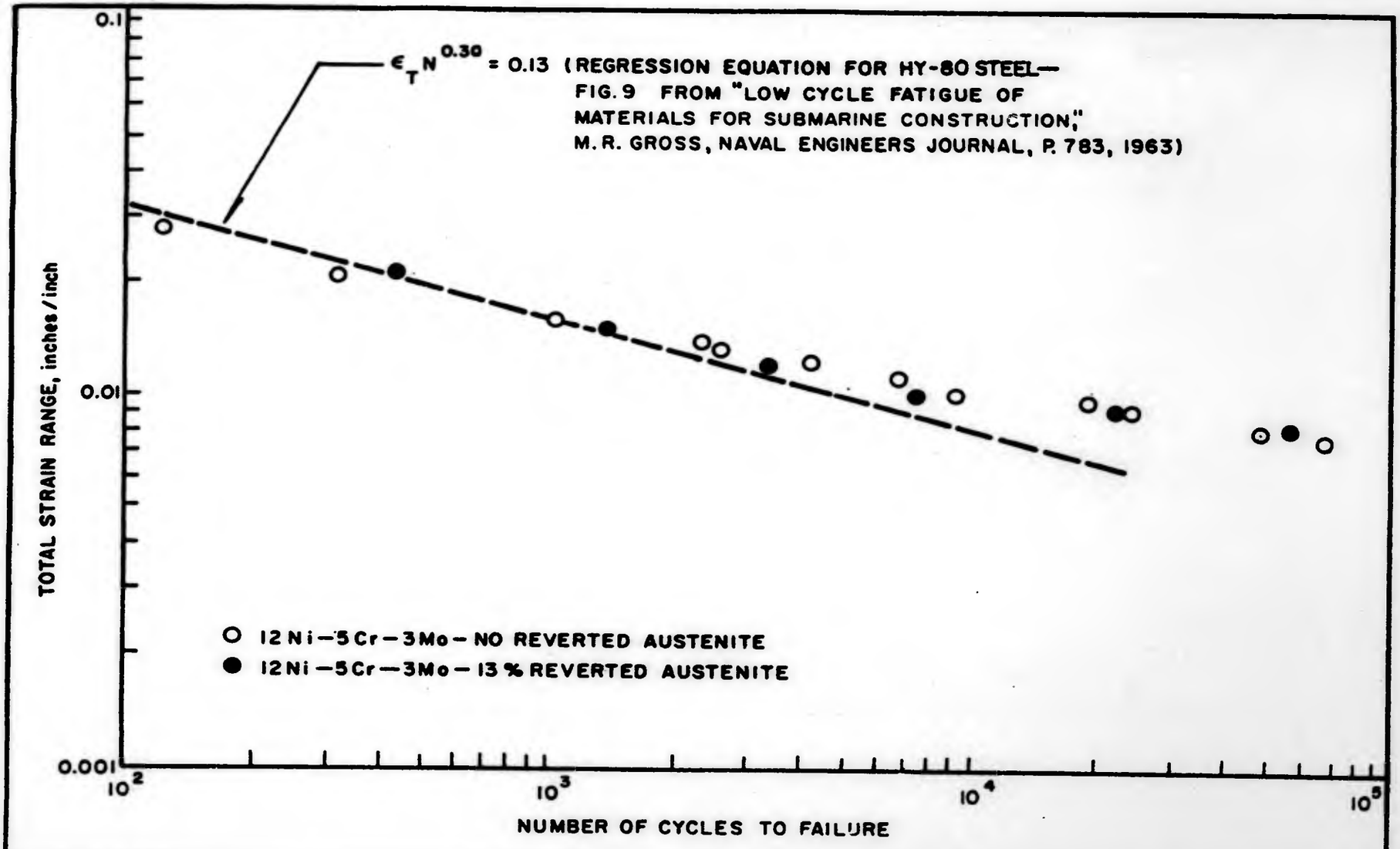

EFFECT OF 13 PERCENT REVERTED AUSTENITE ON FATIGUE BEHAVIOR OF 12 Ni–5Cr-3Mo STEEL

DRAWN BY	CHK'D BY	APPROVED BY	UNITED STATES STEEL CORPORATION	FIGURE NO.
G.A.Z.	S.T.R.	J. H. G.	APPLIED RESEARCH	5
DRAWING No		PROJECT No	PITTSBURGH, PA.	
ARL-18-416		40.018–001 (37)		
		DATE 11/11/64		

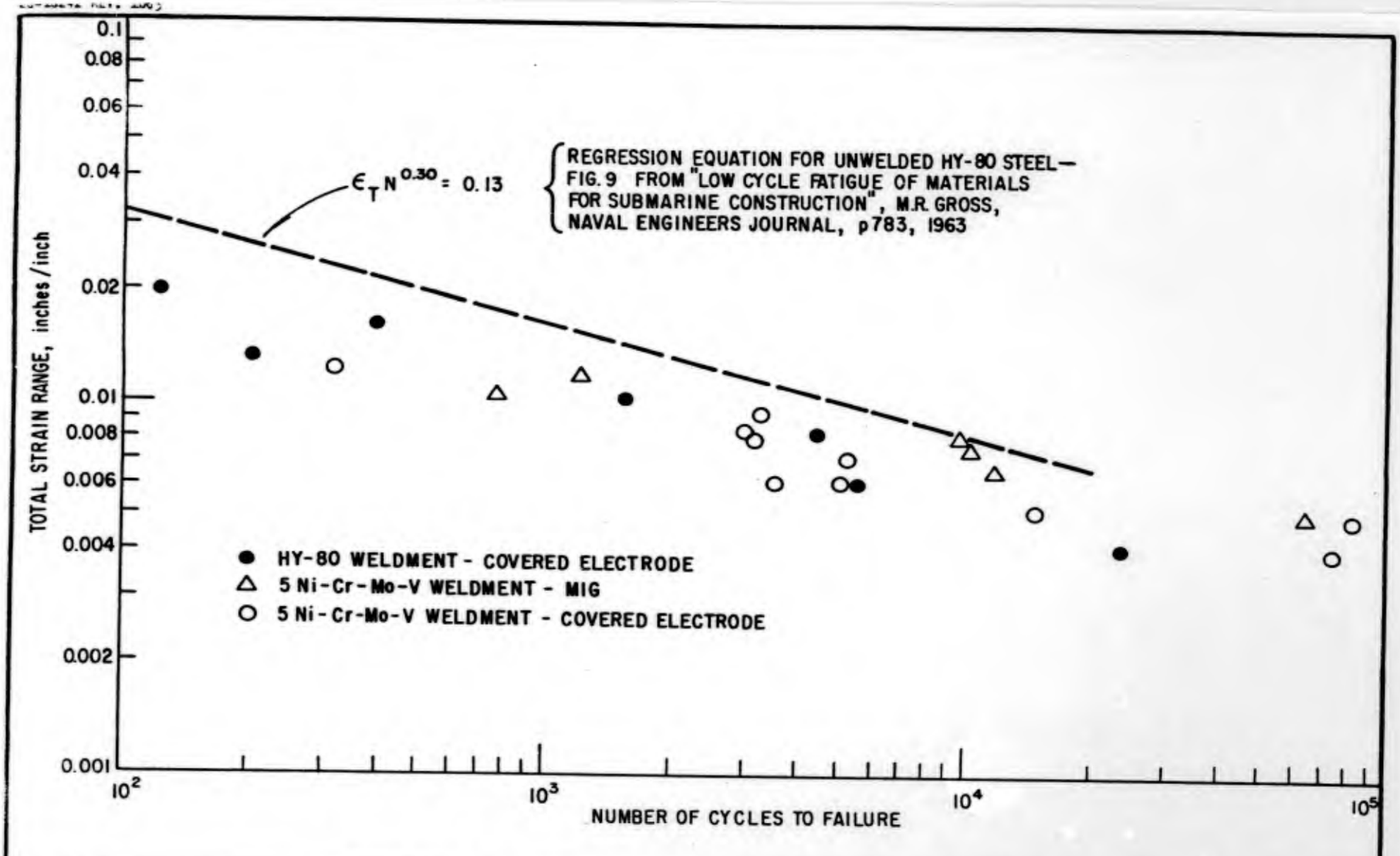

LOW-CYCLE FATIGUE RESULTS FOR 5 Ni-Cr-Mo-V WELDMENTS AND HY-80 WELDMENTS

DRAWN BY	CHK'D BY	APPROVED BY
M.M.	S.T.R.	J.H.G.
DRAWING No.		PROJECT No.
ARL 18-428		40.018-001 (37)
		DATE 11/11/64

UNITED STATES STEEL CORPORATION
APPLIED RESEARCH
PITTSBURGH, PA.

FIGURE NO. 6

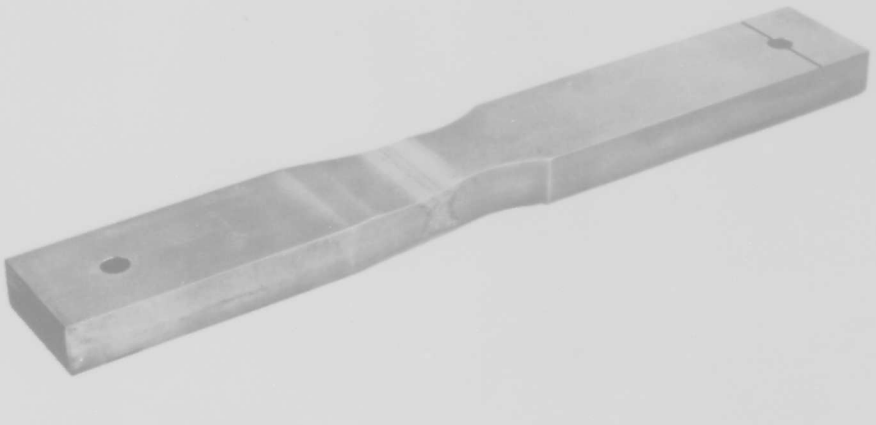

A. Over-all specimen (1 x 2-1/2 x 18 inches).

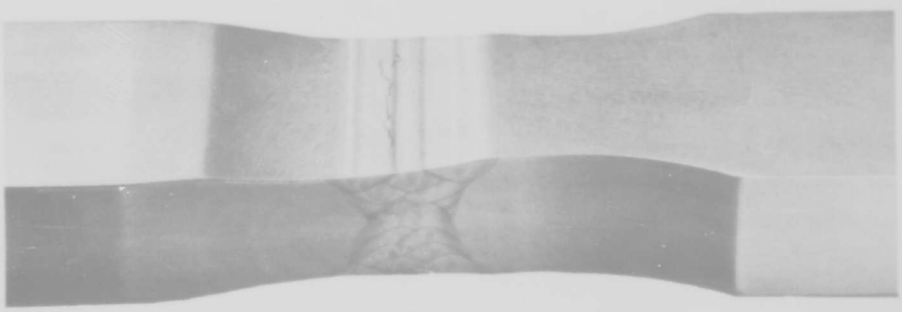

B. Close-up of weld showing crack location.

Figure 7. Tapered welded low-cycle fatigue specimen.

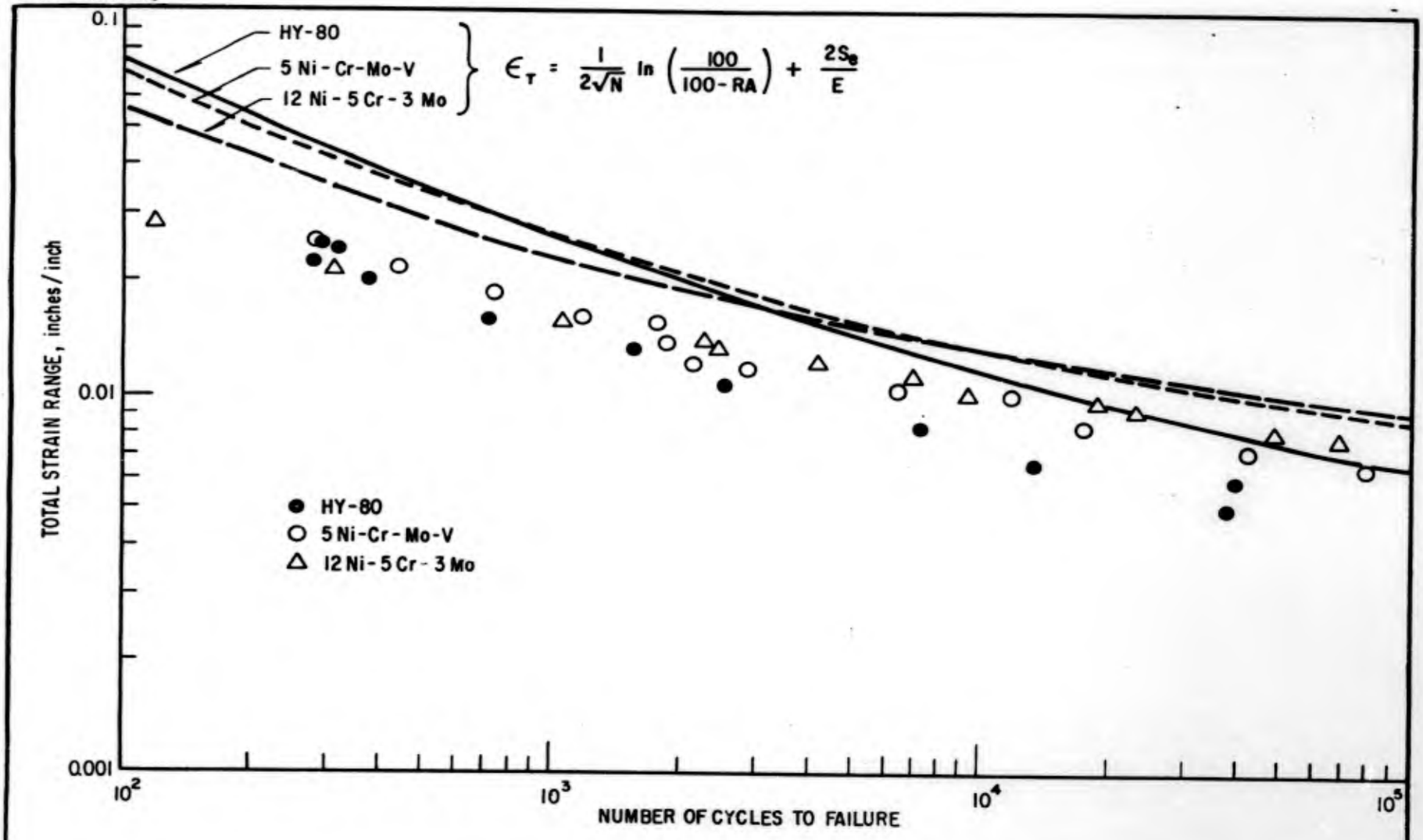

FATIGUE DATA ANALYZED WITH LANGER'S[4] EQUATION

DRAWN BY	CHK'D BY	APPROVED BY	UNITED STATES STEEL CORPORATION	FIGURE NO.
M.M.	S.T.R.	J. H. G.	APPLIED RESEARCH	
DRAWING NO		PROJECT No. 40.018-001(37)	PITTSBURGH, PA.	8
ARL 18-475		DATE 11/11/64		

1025 Clearprint Pitt Photo Litho Co., Inc. Pgh., Pa.

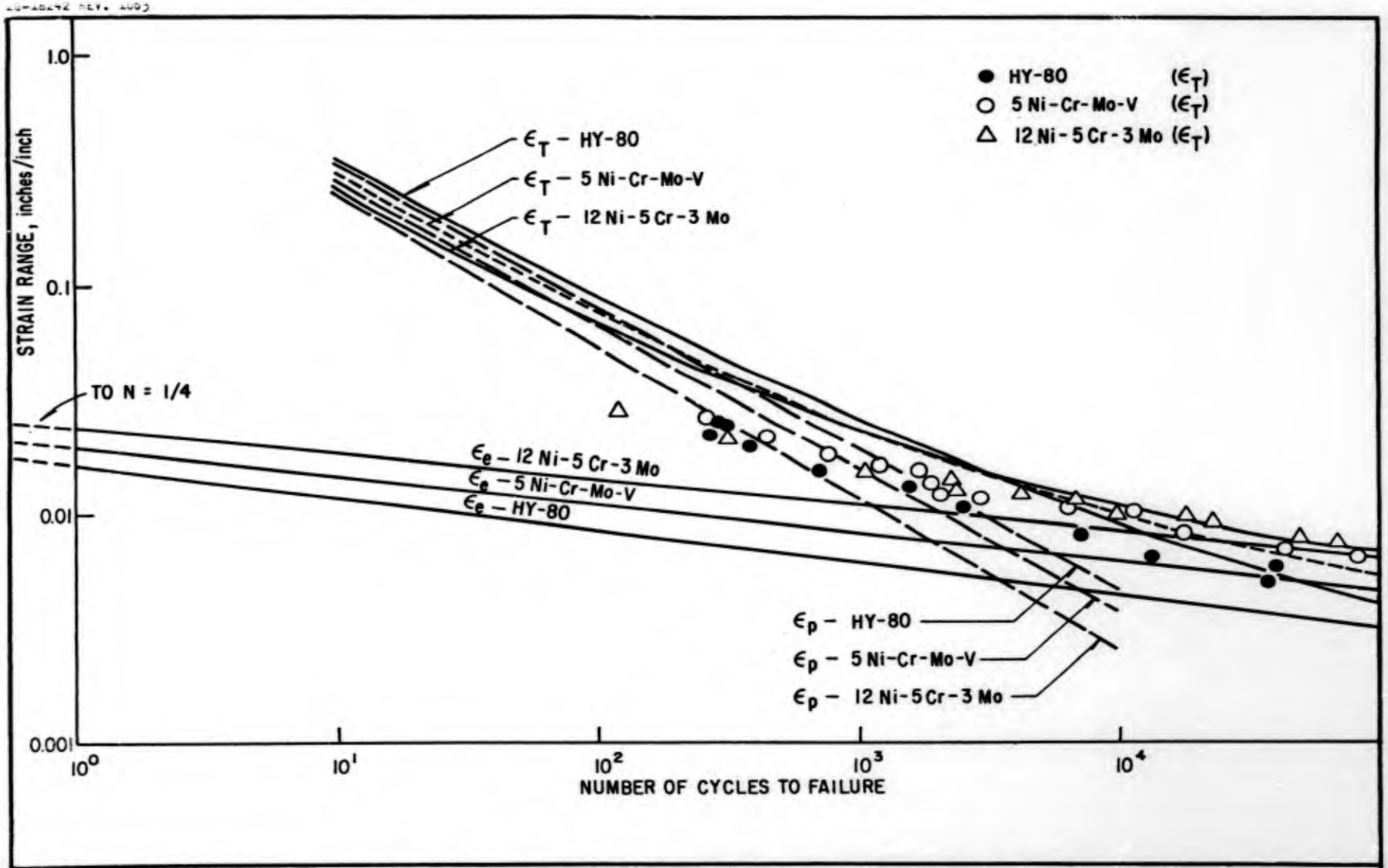

FATIGUE DATA ANALYZED WITH MANSON'S[5] EQUATIONS

DRAWN BY	CHK'D BY	APPROVED BY	UNITED STATES STEEL CORPORATION	FIGURE NO.
M.M.	S.T.R.	J.H.G.	APPLIED RESEARCH	
DRAWING NO		PROJECT No 40.018-001(37)	PITTSBURGH, PA.	
ARL 18-476		DATE 11/13/64		9

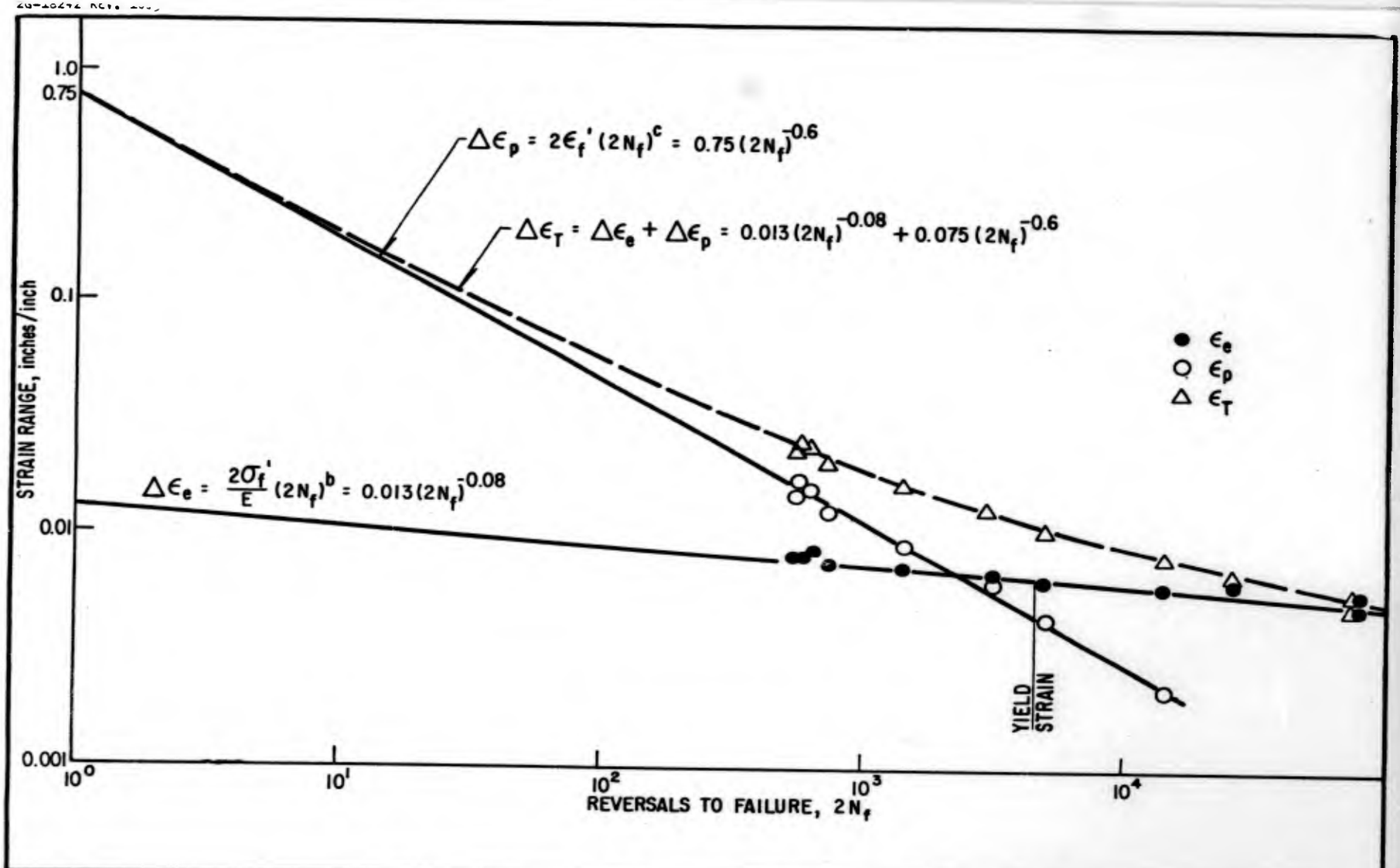

HY-80 STEEL DATA ANALYZED WITH MORROW'S[61] EQUATIONS

DRAWN BY	CHK'D BY	APPROVED BY	UNITED STATES STEEL CORPORATION	FIGURE NO.
M.M.	S.T.R.	J. H.G.	APPLIED RESEARCH	
DRAWING No		PROJECT No	PITTSBURGH, PA.	
ARL 18-477		40.018-001 (37)		10
		DATE 11/12/64		

1025 Clearprint Pitt Photo Litho Co., Inc. Pgh., Pa.

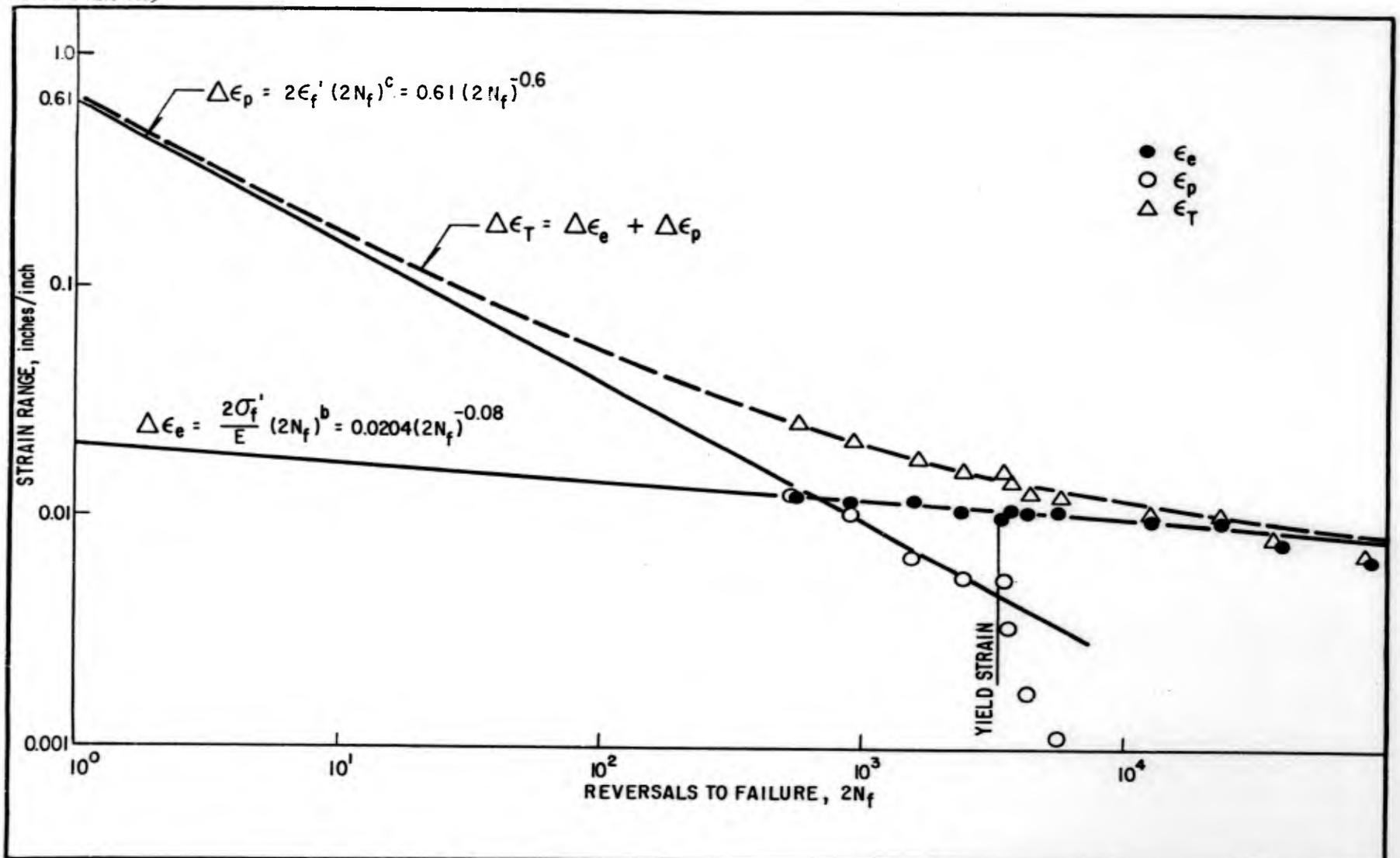

5 Ni-Cr-Mo-V STEEL DATA ANALYZED WITH MORROW'S[6] EQUATIONS

DRAWN BY	CHK'D BY	APPROVED BY	UNITED STATES STEEL CORPORATION	FIGURE NO.
M.M.	S.T.R.	J.H.G.	APPLIED RESEARCH	
DRAWING NO		PROJECT NO 40.018-001 (37)	PITTSBURGH, PA.	11
ARL 18-478		DATE 11/13/64		

1025 Clearprint Pitt Photo Litho Co., Inc. Pgh., Pa.

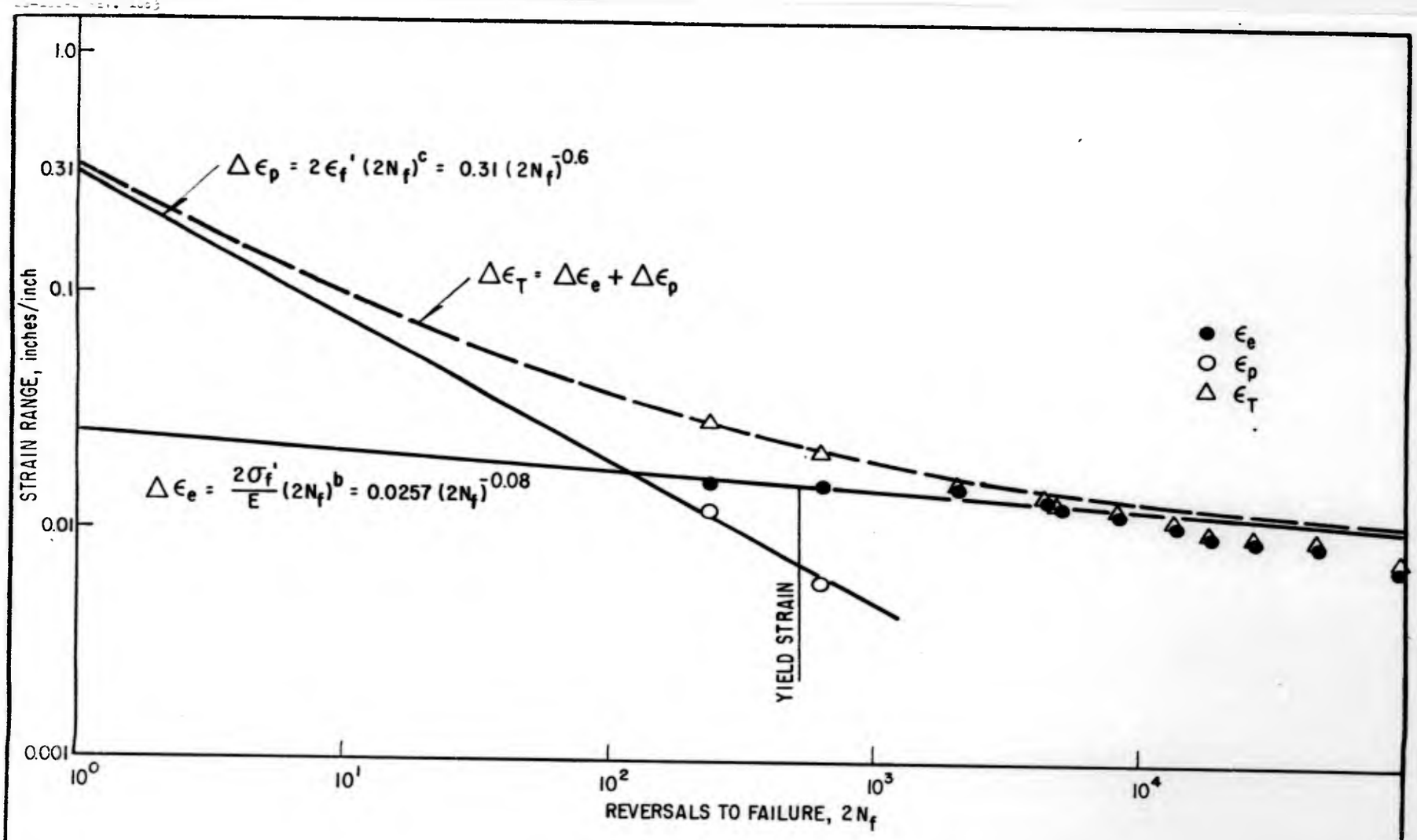

12 Ni-5 Cr-3 Mo STEEL DATA ANALYZED WITH MORROW'S[6] EQUATIONS

DRAWN BY	CHK'D BY	APPROVED BY
M.M.	S.T.R.	J.H.G.
DRAWING NO.		PROJECT NO.
ARL 18-479		40.018-001(37)
		DATE
		11/13/64

UNITED STATES STEEL CORPORATION
APPLIED RESEARCH
PITTSBURGH, PA.

FIGURE NO. 12

UNCLASSIFIED